Response to reviewers

A sparse reconstruction method for the estimation of multiresolution emission fields via atmospheric inversion

Ray, Lee, Yadav, Lefantzi, Michalak and van Bloemen Waanders, GMDD 7:5623-5659, 2014.

The new manuscript, marked-up via latexdiff, has been appended to this response document. Edits in the manuscript are referred to in the response in red, within [brackets]

Response to Reviewer No. 1

We thank the reviewer for his/her suggestions and comments. Our responses to his/her suggestions are below.

Overall response: At the very outset we would like to clarify that our study is focused on investigating the algorithmic aspects of a sparse reconstruction method (based on Stagewise Orthogonal Matching Pursuit, StOMP) for estimating rough emission fields, such as that of fossil-fuel CO2 (ffCO2). A sparse reconstruction method is necessary since the spatial parameterization for rough fields tends to be high dimensional (many parameters). The parameters that can be estimated depend on the information content of the observation data, which can change with time/season. The method is not customized to a particular tracer, measurement network or a transport model. Customization to a tracer occurs when we choose a spatial parameterization (a wavelet-based random field model in this study) for use with our sparse reconstruction method. It also occurs when we choose an observational dataset. The method can accommodate prior information on the field being estimated, but only uses its spatial pattern; thus, by design, it is insensitive to under/overestimation of the emissions in the prior information.

The paper investigates which formulations of the inverse problem do and do not work, and explains why. It develops a metric (mutual coherence) to quantify the information content in the observations collected by our measurement network. It finds the information content lacking, which motivates the need to introduce prior information into the inverse problem. We then identify a way to do so; the obvious/intuitive ways do not work. We also show how a wavelet-based field model, designed for modeling fields in rectangular geometries, can be used to estimate emission fields in an irregular region $\mathcal{R}$ (the Lower 48 states of the US). Finally, we show how StOMP can be extended to enforce non-negativity on the estimates. Sparse reconstruction methods are typically not used in atmospheric inversions.

Our motivation to develop this method arose from a need to construct and/or validate gridded inventories of ffCO2. Fortunately, many gridded ffCO2 inventories are available and a wavelet-based spatial parameterization also exists. We demonstrated the method in an idealized, synthetic-data inversion. The idealizations include: (1) assuming ffCO2 to be a radiocarbon-like tracer and ignoring interference by biospheric CO2 which can make ffCO2 estimation impossible except in winter (see Shiga et al., [2014]); (2) using a model-data mismatch ε that is smaller than the one used in real-data inversions and (3) assuming the same distribution for ε for all towers (i.e., ignoring transport model errors). These

idealizations allowed us to explore issues related to the algorithm and formulations in a relatively "clean" setting. We also use an observational dataset collected from a measurement network that was sited with biospheric CO2 fluxes, not ffCO2, in mind (the towers are usually far from locations with high ffCO2 emissions); a network for ffCO2 does not currently exist.

Due to these idealizations adopted in our test, we do not claim that the method can be used to estimate ffCO2 emissions fields in a realistic setting using measurement techniques and infrastructure that are currently available (or could be in the near future). At the very least, our method has to be extended to include the estimation of biospheric fluxes as well as larger and tower-dependent model – data mismatches. This is a substantial body of work and outside the scope of this study. In order to check how accurate the estimates would be, we would have to conduct an OSSE (Observational System Simulation Experiment) or design an ideal network. Our tests also provide no information on the best method to collect information on estimation of ffCO2 emissions over regional scales (tower, airplane transects etc.).

We check our inversion method using the following metrics:

1. As part of our algorithmic development, we modify StOMP to incorporate prior information to improve estimates. We check whether it indeed does so, since the information content of the observations are found to be poor.
2. The aim of sparse reconstruction is to estimate parameters that are supported by data (usually large spatial patterns in the emission field) and remove the details that are not. We check whether this "sparsification" characteristic of the algorithm is still present after including prior information.
3. Our method restricts emission fields in an irregular region $\mathcal{R}$ (while using a wavelet-based model); this incurs a computational cost that can be limited by a user-defined setting. We check if the behavior of the algorithm provides a principled way of computing that setting (e.g., if improvement of results shows a "diminishing returns" behavior with the computational cost).

Note that in this study we do not use the accuracy of the estimated emission fields as a metric for evaluating our inversion method. This is because accuracy of estimation is determined primarily by two factors (once we have specified a model – data mismatch): (1) the suitability of the spatial parameterization for the rough fields being estimated and (2) the information content of the observational dataset. In our previous paper Ray et al, [2014] we fixed the observational data and used the accuracy of the emission estimates to gauge the quality of the spatial parameterization. The converse procedure – fixing the spatial parameterization and varying the quantity of observational data – is not a very useful direction for investigation, for our StOMP-based method, because of the following reasons:

1. The estimation accuracy of StOMP, as the quantity of observational data is varied, has been investigated in Donoho et al, [2012]
2. If the aim is to obtain a very accurate reconstruction of the ffCO2 field (when we have full discretion to design an ideal observation network/technique), then we are limited only by what the spatial parameterization can capture. As reported in our previous paper [Ray et al, 2014], the spatial parameterization with 1023 wavelet coefficients (parameters) has a relative error of 10% at the 1-degree resolution; this would be recovered (modulo the small model – data mismatch) in case of an ideal network. If we retain all wavelet coefficients that can be described on a 1-degree mesh in the spatial

parameterization (4096 coefficients), the reconstruction will be perfect (modulo the model – data mismatch).

Atmospheric inversion could be a way of estimating/verifying self-reported ffCO2 emissions in countries where the uncertainty is high. The uncertainty in emission reports from China is estimated to be 15-20% [Andres et al, 2012], though studies based on the TRACE-P campaign proposed a 54% revision of inventory estimates for 2000 [Suntharalingam et al, 2004] (it was officially revised upwards by 23% between 2006-2007). Other countries have larger variations. These uncertainties affect inventories, but do not affect our inversion method (see paragraph 1). Even if our variable of interest were to be total emissions over a region (nation or province), estimating a spatially variable emission field before spatially aggregating it reduces the aggregation error. However in order to do this, a measurement infrastructure designed with ffCO2 in mind is a requirement. Its size will be determined by whether we are interested estimating total national emissions or we seek fine scale details.

In addition, as mentioned above, our method can be used with other tracers provided we have a spatial parameterization for them.

The introduction section in our paper does not describe the idealized nature of our tests or the limits/caveats on the conclusions that can be drawn from them. It also does not describe the reasoning behind the metrics that were adopted for evaluating our algorithm. We will add them in the revised paper. [Pg7:26 – Pg9:25; Pg29:13 – Pg29:24]

Overarching comments

The reviewer states his/her first general issue –"Accessibility: Much of the paper uses very technical wording, and I worry that much of this phrasing may not be very accessible to atmospheric scientists. Most existing atmospheric inversion studies use a single framework for inverse modeling – Eq. 1 listed in this article. Additional frameworks, like the one presented in this article, could be incredibly useful. However, I suspect that most atmospheric scientists will be unfamiliar with this type of sparse reconstruction in the same way that most are familiar with Eq. 1. I might focus on making this article more accessible to that audience. The authors could do this in a number of ways: (1) by removing technical phrases or terms of art that are not strictly necessary, (2) by providing more descriptive explanation of some of the methods, or (3) by more explicitly guiding the reader through some of the equations.

In particular, I might focus on re-wording the abstract and introduction in a less technical way – in a manner that provides more physical intuition for a reader who may not be familiar with this type of sparse reconstruction method. This re-wording would help broaden the article's appeal to a wider audience and will clearly motivate the subsequent sections that, by necessity, are more technical. To this end, I might focus on giving the reader a holistic, descriptive overview of why under-constrained problems can be challenging, what sparse reconstruction methods are, and how those methods can provide an attractive solution."

We will re-write the abstract to be simpler and jargon-free (as far as possible). We will include a paragraph on how sparse reconstruction methods help in the solution of inverse problems. [Pg4:17 – 22]

The reviewer states his/her second general issue – "I am somewhat concerned about the choice of synthetic data study. A recent paper by Shiga et al. (2014,

doi:10.1002/2014GL059684) indicates that existing atmospheric measurements have difficulty identifying ffCO2 fluxes above biospheric fluxes. As a result, I wonder if ffCO2 is necessarily the best species for a synthetic case study. In the real world, these emissions are often obscured by fluxes from the biosphere. The authors might instead want to consider a gas with both natural and anthropogenic emissions that are largely non-negative. For example, methane, nitrous oxide, or one of several fluorinated greenhouse gases could make for a good synthetic case study.

I think this issue may actually be cursory to the central objective of the paper – to present a new inversion method. However, it may nonetheless distract the reader or detract from the perceived applicability of the method."

We agree that idealizations we adopted for in our test case (no biospheric CO2 fluxes, very small model-data mismatch etc.) could distract readers (especially in view of Shiga et al.'s recent paper), even though they may be tangential to the usefulness and novelty of a sparse reconstruction method in atmospheric inversion. See "Overall response" for the reasons behind our use of the idealizations.

However, we did investigate other pollutants and ultimately decided on ffCO2. Our choice of ffCO2 (in our idealized inversion) was based on the fact that we had the spatial parameterization for ffCO2 ready (unlike the other gases). Further, anthropogenic CH4 and N2O emissions also suffer interference from their natural counterparts (about 40% and 70% of the total respectively). Lastly, the issues related to ffCO2 (scientific, economic and political) are well known, which allowed us to describe them in a concise manner, and devote most of the paper to mathematical and algorithmic issues.

Detailed comments

1. The reviewer states "The beginning of the abstract is somewhat technical and may be challenging for the reader to follow. For example, the terms "wavelet-based random field models" and "non-rectangular geometries" may not be familiar to the reader. The authors could instead open with a non-technical sentence that communicates how this sparse reconstruction scheme is advantageous or how it represents advancement."

We will re-write the abstract [see abstract]

2. Pg 5625, Line 6-8: The reviewer asks "Would it be possible to cite a reference that illustrates an example of this?" i.e. whether we could cite a reference that shows that non-stationary fields cannot be modeled using multivariate Gaussian fields

We will re-write this sentence. Non-stationary fields can be modeled using multivariate Gaussian fields but require complex covariance models. In practice, these are difficult to construct and we adopt a model (typically, a variogram) that has one length-scale. Such a model suffices if the emission fields being modeled are smooth. In some cases, a non-stationary field can be represented as a non-stationary mean field with an additive correction modeled as a stationary multivariate Gaussian field. In such a case, modeling effort shifts to constructing the mean field representation.

We will add this clarification in the text. [Pg3:19 - 20]

3. Pg. 5625, Line 16-17: The reviewer asks "Could one theoretically use a model selection method (like AIC, BIC, or DIC) to decide whether a parameterization is too simple or too complex?"

Yes, one could start with an over-parameterized model, create multiple variations of it by retaining a subset of the parameters and use AIC (or BIC or DIC) to choose the best model after fitting to data. It is an alternative to sparse reconstruction to simplify the spatial parameterization, conditioned on data.

We have added this explanation in the paper. [Pg4: 3 - 4]

4. Pg. 5625, Line 25-28: The reviewer points out "These examples add a lot of extra technical detail to the description of sparse reconstruction methods. I wonder if this level of detail is necessary when giving the reader a broad, holistic definition of sparse reconstruction."

Our method for estimating ffCO2 involves formulating a linear inverse problem in a way that could be solved using StOMP. Since StOMP is so central to our method we felt that it would be natural to introduce it early when discussing what sparse reconstruction methods are and what they do. The other methods cited (Matching Pursuit and its variations) are all related to StOMP and identify the class of sparse reconstruction methods we will use.

Note that there are other l_1 minimization methods such as LASSO (Least Absolute Shrinkage and Selection Operator) and LARS (Least Angle RegreSsion) that can also solve the sparse reconstruction problem. Since we will not be using this "family" of algorithms in our paper, we have omitted them from our brief introduction to sparse reconstruction methods. Sparse reconstruction (or shrinkage regression) is too large a topic to be adequately summarized in our paper.

5. Pg 5626, Lines 2-6: The reviewer asks: "What is an l1 and l2 norm? Furthermore, what is the "offline construction of a spatial parameterization" and why would we want to dispense of it?"

l_1 norm of $\mathbf{x} = \|\vec{x}\|_1 = \sum|x_i|$. l_2 norm of $\mathbf{x} = \|\vec{x}\|_2 = \sum_i x_i^2$. We will add this definition in the text. [Pg4: 17 - 18]

The conventional way of estimating a field is as follows:

1. *Determine a model for the field ("spatial parameterization")*: It could be based on Gaussian Process (or Gaussian random fields) in which case one develops a model for the field's mean as well as a covariance model for deviations from the mean field model. Alternatively, one could opt for a field model constructed as a linear sum of orthogonal bases (wavelets, eigenvectors of the covariance matrix etc.), in which case one decides on which bases to retain in the field model. There are many methods to do so. This is the "offline construction of the spatial parameterization".
2. *Solving the inverse problem:* Here one fits the spatial parameterization to the observed data using whatever method is convenient.
3. *Refining the model:* The spatial model constructed could be too complex or too simple for the observations used to solve the inverse problem. To address this, one proposes a set of competing spatial parameterizations and solves the inverse problem again. Thereafter, using a metric such as AIC, one picks the best spatial parameterization, which provides accuracy without overfitting the data. This is an

iterative process, since the proposed set of competing spatial parameterizations could very well be incomplete.

4. *Repeat if the quality of the data is time-dependent:* We estimate weekly emission fields for a year. Since wind directions change with time, the information content of the observations (the "quality" of the observations) is time-dependent. The process described above has to be repeated for every week. This is tedious.

Consequently, we were motivated to construct a method where we could dispense with the offline construction of the spatial parameterization. Rather, we desired a method where we could start with a spatial parameterization that had too many parameters and have the sparse reconstruction algorithm identify, given the observations available, the parameters that could actually be estimated (and set the rest to zero). Our sparse reconstruction method does this efficiently. The set of "estimate-able" parameters could vary week to week. One could call this process an "online construction of a sparse spatial parameterization" or "online sparsification of the spatial parameterization".

6. Page 5626, Line 19-20: The reviewer asks, "What do you mean by the choice of the proxy used for spatial disaggregation"?

Most fossil-fuel fuel CO2 emission inventories are constructed by obtaining fossil-fuel emissions declared by a country (only national and/or regional aggregate emissions are provided) and disaggregating them down to much finer resolutions e.g. 10km. This spatial disaggregation/downscaling is performed using a proxy of human activity that is available at such a fine spatial scale. To date, population density, measures of economic activity (e.g., per capita GDP) and images of lights at night have been used as the disaggregation / downscaling proxies. These proxies are quite different at fine spatial scales and these differences are naturally manifest in the downscaled emissions. Consequently, the ffCO2 inventories do not agree at fine spatial scales.

7. Page 5627, Line 12-13: The reviewer asks "What is a wavelet-based random field model?"

Wavelets are an orthogonal basis set. Any function (e.g. emission field) defined on a grid with N gridcells can be decomposed (by projection) on the N wavelets that can be described on the grid. Not all projections are large/numerically significant, and consequently the function could be approximated by a weighted linear combination of k wavelets, $k << N$. This creates a wavelet-based field model.

The k weights constituting the wavelet-based field model can be considered to be random numbers. Depending on the values assumed by the weights, we can create an infinite number of fields ("random fields"). However, since these fields are constructed only using k wavelets on an N grid-cell grid, they fall in a certain class of fields i.e., we cannot create all fields that could be described on the grid. This is called a wavelet-based *random* field model.

We will add this description in the paper. [Pg6: 6 – 12]

8. Pg 5627, Line 22-23: The reviewer asks "What kind of a spatial parameterization does this paper develop? i.e. it is not clear what the term "spatial parameterization refers to here".

The parameterization refers to a spatial parameterization that was developed in our previous work (we begin the sentence with a citation of our previous work). It is a wavelet-

based random field model, constructed out of Haar wavelets, for representing ffCO2 emissions. The wavelets retained in the model were selected by projecting radiances of lights at night on to a set of Haar wavelets described on a 1 degree X 1 degree grid; only about 25% of the wavelets were retained. The weights of the wavelets are deemed to be random numbers (uniformly distributed between plus and minus infinity) and are estimated by the inverse problem that we describe in this paper.

We will add this description of what we mean by spatial parameterization in the manuscript. [Pg5:21 - 25]

9. Pg 5629, Line 4-11: The reviewer asks "How different are EDGAR and Vulcan? This difference would help the reader understand whether the estimated emissions shown in Fig. 1 more closely resemble the prior (EDGAR) or the true fluxes (Vulcan). The authors may want to consider adding a plot of EDGAR fluxes to Fig. 1."

EDGAR emissions are 7.1% higher than Vulcan emissions when aggregated over the US. The RMSE between the two is 0.035 μmoles $m^{-2}s^{-1}$ of C and the Pearson correlation between the two is 0.726.

We will add a figure of EDGAR emissions to the text. Remember, though, that Vulcan emissions change with time while EDGAR is an annual average. [Fig. 1 in updated manuscript]

10. Pg 5630, Eq. 1 The reviewer ask "It may be useful to the reader to define the dimensions of each matrix or vector."

Updated in the new manuscript. [Pg10: 9 – 11]

11. Pg. 5630, Line 26: The reviewer asks "What are orthogonal bases with compact support? Some readers may understand this term, but I worry that many atmospheric scientists may not fully understand this technical term."

Orthogonal bases are a set of functions, which are mutually orthogonal i.e. they have zero projection on each other, in the domain where they are defined. Sine waves are a common example. Because of orthogonality, they can be linearly combined to model arbitrary functions.

Compact support refers to the fact that the bases are non-zero only in a part of the domain where they are described. This is unlike sine functions that are defined between plus/minus infinity. Wavelets are orthogonal and have limited support. The limited spatial extent of the basis allows us to use them to define localized structures and discontinuities with ease, unlike sine waves.

We will add this description of orthogonal bases with compact support in the manuscript. [Pg11:13 – 17]

12. Pg 5631, Eq 3. The reviewer asks "It might be useful to the reader to explain in words what the components of this equation mean. I.e., it may be helpful to guide the reader through this equation. The current text does not provide much explanation of what this equation means. In addition, does μ refer to the mean here?"

We will do so in the updated manuscript. [Pg12: 13 - 16]

13. Pg 5631: The reviewer asks "Are "incoherence" and "mutual coherence" the same thing? It may be useful to explain the relationship of these terms to the reader."

No, quite the opposite. Zero mutual coherence is (perfect) incoherence. Loosely, we refer to a small mutual coherence (small compared to $N^{1/2}$) as "incoherence".

We've clarified this in the new manuscript. [Pg12:19]

14. *Pg. 5632, Line 11: The reviewer asks "What is the l0 norm of $\vec{w}$ and what is the l2 norm of the measurement-model discrepancy? Do they refer to the "1" and "2" subscripts in Eq. 4? If so, it may be useful to clarify here."*

l_0 norm of w = $\|w\|_0 = \sum_i w_i^0$ = the number of non-zero elements in vector **w**. The l_2 norm has been described in Response no. 5. It is indeed the "2" subscript in Eq. 4. The "1" subscript refers to l_1 norm (see Response 5 above).

15. Pg 5635, Eq. 7: The reviewer states "Is there any way to guide the reader through this equation? I know that this equation is, to some degree, an extension of Eq. 6, but I worry that the authors may lose the reader here."

We will do so. It was described much better in our previous paper (which had the full context within which it was developed), but we realize that the current paper has to stand on its own. [Pg16:8—10]

16. Pg 5637, Line 3-6: The reviewer asks "What is the ultimate effect of fine versus coarse wavelets? i.e., what effect would these differences have on the estimated fluxes or what desirable quality would these properties confer?"

The coarse wavelets capture the large-scale patterns in the emission field e.g., the urban sprawl on the East Coast whereas the fine wavelets capture local structures e.g. intense regions of ffCO2 emissions like cities in the High Desert e.g., Salt Lake City. As mentioned in the paper, it is easy to estimate the emission in the sprawl as a number of measurement towers lie inside it. On the other hand, an isolated hot spot like Salt Lake City can be difficult to estimate unless it lies close to a tower.

17. Pg 5637: The reviewer asks "Approach C: Could you potentially describe in more qualitative terms how this approach differs from B?"

Approach B models the true emission as essentially our prior belief (based on EDGAR) with an additive correction field ΔF. This is an intuitive way of modeling the emission field, but leads to problems when using sparse reconstruction.

Approach C normalizes the wavelet coefficients of the emission field being estimated using the wavelet coefficients from the prior (EDGAR). This works well.

We will add this explanation in the updated manuscript. [Pg18:10 – Pg19:22]

The reason for the failure of Approach B is explained on Pg 5641, Line 22:28 and Response 16. It arises from the fact that wavelets with smaller support (fine wavelets) have wavelet weights (or wavelet coefficients) that are large – they tend to model isolated emission sources or abrupt changes in the emission field. When we model the emissions with a correction over EDGAR, the wavelet coefficients of correction, corresponding to the fine wavelets, also tend to be large. Since the sparse reconstruction method seeks to reduce $l_1(\Delta w)$, where Δw are the wavelet coefficients of the correction field, the large coefficients of the fine wavelets quickly come under scrutiny. Unless they can induce a large change in predicted concentrations at the measurement towers (only possible if there's one nearby), they are quickly removed. In fact, Δw becomes very sparse indeed, and the estimated emission field looks a lot like EDGAR.

The reason for this discrepancy is the l_1 (**w**) minimization implicitly assumes that all elements of **w** are of the same order of magnitude. In our problem, they are not.

Consequently, in Approach C we normalize the wavelet coefficients of the modeled field with that of the prior emission field. It renders the wavelet coefficients non-dimensional and the same order of magnitude. The sparse reconstruction proceeds as expected. However, in normalizing, we have assumed that the prior's wavelet coefficients' proportions to each other are similar to those of the true emission field's wavelet coefficients. This implies that normalized wavelet coefficients are non-dimensional and of the same order of magnitude, though not necessarily O(1). If the prior is not a gross under/over-estimate of the true emissions, the normalized wavelet coefficients are of O(1), in addition. Thus Approach C provides a way of incorporating prior information. This is explained on Pg. 5643, Line 17:24.

18. Pg 5638 Eq. 11 The reviewer asks "Have these variables already been defined elsewhere in the manuscript? I may have missed this definition. If not, it would be helpful to explicitly define these variables for the reader (or explicitly state how they relate to the equations in Approaches A-C)."

This is our mistake – they have not been defined. We will fix this in our updated manuscript. [Pg 19, below Eq. 13]

19. The reviewer states "The authors do a great job of leading the reader through this section in a structured and informative way"

20. The reviewer states "Conclusions: The conclusion section is well written. The authors are adept at summarizing their method and its advantages in a way that is likely to be accessive to many readers

Thank you!

21. Pg. 5648 Line 3-8: The reviewer asks "The authors may want to remind the reader which sections discuss each step. The reader may not remember each step exactly, and a reference to individual sections would help the reader jump to this information quickly."

The paragraph describes a test that we did (it involved omitting certain steps in the inversion method) and whose results are not presented in the paper. However, we will refer back to the sections as we describe the steps that were omitted, leading to the failure of the

tests.

We will add this clarification in the updated manuscript. [Pg29:26 - 28]

22. Pg 5648, Line 11: The reviewer asks "How would a Kalman filter rectify this problem? I would either clarify this logic or omit the statement."

Using a Kalman filter (or probably an ensemble Kalman filter, given the large dimensionality) would provide us with a mean emission field and a covariance matrix. The covariance matrix would allow us to compute standard deviations on the estimated fields.

23. Pg. 5648, Line 17:20: The reviewer states "I think this Matlab code will make the inversion method much more accessible to most readers."

We agree, and we are pleased to announce that we have finally received permission to distribute the code. The software has been freely downloadable on the website since October 10th.

24. The reviewer states "Figure 1: I might set zero values to white or use a color scale that uses light colors or shades for low emissions values. This could make the figure more visually appealing and easy to see."

We will do so.

25. The reviewer states "Figure 5: It could be more informative to list actual dates on the x-axis in panel a. The current label ("observation number") is not very informative to the reader."

We will do so.

References

[Andres et al, 2012] R. J. Andres et al, "A synthesis of carbon dioxide emissions from fossil-fuel combustion", Biogeosciences, 9, 1845-1871, 2012. doi: 10.5194/bg-9-1845-2012.

[Donoho et al, 2013] D. Donoho et al, "Sparse solutions of underdetermined linear equations by Stagewise Orthogonal Matching Pursuit", IEEE Transactions on Information Theory, 58, 1094-1121, 2012.

[Ray et al, 2014] J. Ray et al, "A multiresolution spatial parameterization for the estimation of fossil-fuel carbon dioxide emissions via atmospheric inversions", Geoscientific Model Development, Geosci. Model Dev., 7, 1901-1918, 2014. doi:10.5194/gmd-7-1901-2014.

[Shiga et al, 2014] Y. P. Shiga et al, "Detecting fossil fuel emissions patterns from sub-continental regions using North American in-situ CO2 measurements", Geophysical Research Letters, 41(12):4381-4388, 2014.

[Suntharalingam et al, 2004] P. Suntharalingam et al, "Improved quantification of Chinese carbon fluxes using CO2/CO correlations in Asian outflows", Journal of Geophysical Research, 109, D18S18, 2004. doi:10.1029/2003JD004362.

Response to reviewers

A sparse reconstruction method for the estimation of multiresolution emission fields via atmospheric inversion

Ray, Lee, Yadav, Lefantzi, Michalak and van Bloemen Waanders, GMDD 7:5623-5659, 2014.

Response to Reviewer No. 2

We thank the reviewer for his/her suggestions and comments. Our responses to his/her suggestions are below.

Overall response: At the very outset we would like to clarify that our study is focused on investigating the algorithmic aspects of a sparse reconstruction method (based on Stagewise Orthogonal Matching Pursuit, StOMP) for estimating rough emission fields, such as that of fossil-fuel CO2 (ffCO2). A sparse reconstruction method is necessary since the spatial parameterization for rough fields tends to be high dimensional (many parameters). The parameters that can be estimated depend on the information content of the observation data, which can change with time/season. The method is not customized to a particular tracer, measurement network or a transport model. Customization to a tracer occurs when we choose a spatial parameterization (a wavelet-based random field model in this study) for use with our sparse reconstruction method. It also occurs when we choose an observational dataset. The method can accommodate prior information on the field being estimated, but only uses its spatial pattern; thus, by design, it is insensitive to under/overestimation of the emissions in the prior information.

The paper investigates which formulations of the inverse problem do and do not work, and explains why. It develops a metric (mutual coherence) to quantify the information content in the observations collected by our measurement network. It finds the information content lacking, which motivates the need to introduce prior information into the inverse problem. We then identify a way to do so; the obvious/intuitive ways do not work. We also show how a wavelet-based field model, designed for modeling fields in rectangular geometries, can be used to estimate emission fields in an irregular region $\mathcal{R}$ (the Lower 48 states of the US). Finally, we show how StOMP can be extended to enforce non-negativity on the estimates. Sparse reconstruction methods are typically not used in atmospheric inversions.

Our motivation to develop this method arose from a need to construct and/or validate gridded inventories of ffCO2. Fortunately, many gridded ffCO2 inventories are available and a wavelet-based spatial parameterization also exists. We demonstrated the method in an idealized, synthetic-data inversion. The idealizations include: (1) assuming ffCO2 to be a radiocarbon-like tracer and ignoring interference by biospheric CO2 which can make ffCO2 estimation impossible except in winter (see Shiga et al., [2014]); (2) using a model-data mismatch ε that is smaller than the one used in real-data inversions and (3) assuming the same distribution for ε for all towers (i.e., ignoring transport model errors). These idealizations allowed us to explore issues related to the algorithm and formulations in a relatively "clean" setting. We also use an observational dataset collected from a

measurement network that was sited with biospheric CO2 fluxes, not ffCO2, in mind (the towers are usually far from locations with high ffCO2 emissions); a network for ffCO2 does not currently exist.

Due to these idealizations adopted in our test, we do not claim that the method can be used to estimate ffCO2 emissions fields in a realistic setting using measurement techniques and infrastructure that are currently available (or could be in the near future). At the very least, our method has to be extended to include the estimation of biospheric fluxes as well as larger and tower-dependent model – data mismatches. This is a substantial body of work and outside the scope of this study. In order to check how accurate the estimates would be, we would have to conduct an OSSE (Observational System Simulation Experiment) or design an ideal network. Our tests also provide no information on the best method to collect information on estimation of ffCO2 emissions over regional scales (tower, airplane transects etc.).

We check our inversion method using the following metrics:

1. As part of our algorithmic development, we modify StOMP to incorporate prior information to improve estimates. We check whether it indeed does so, since the information content of the observations are found to be poor.
2. The aim of sparse reconstruction is to estimate parameters that are supported by data (usually large spatial patterns in the emission field) and remove the details that are not. We check whether this "sparsification" characteristic of the algorithm is still present after including prior information.
3. Our method restricts emission fields in an irregular region $\mathcal{R}$ (while using a wavelet-based model); this incurs a computational cost that can be limited by a user-defined setting. We check if the behavior of the algorithm provides a principled way of computing that setting (e.g., if improvement of results shows a "diminishing returns" behavior with the computational cost).

Note that in this study we do not use the accuracy of the estimated emission fields as a metric for evaluating our inversion method. This is because accuracy of estimation is determined primarily by two factors (once we have specified a model – data mismatch): (1) the suitability of the spatial parameterization for the rough fields being estimated and (2) the information content of the observational dataset. In our previous paper [Ray et al, 2014] we fixed the observational data and used the accuracy of the emission estimates to gauge the quality of the spatial parameterization. The converse procedure – fixing the spatial parameterization and varying the quantity of observational data – is not a very useful direction for investigation, for our StOMP-based method, because of the following reasons:

1. The estimation accuracy of StOMP, as the quantity of observational data is varied, has been investigated in Donoho et al, [2012]
2. If the aim is to obtain a very accurate reconstruction of the ffCO2 field (when we have full discretion to design an ideal observation network/technique), then we are limited only by what the spatial parameterization can capture. As reported in our previous paper [Ray et al, 2014], the spatial parameterization with 1023 wavelet coefficients (parameters) has a relative error of 10% at the 1-degree resolution; this would be recovered (modulo the small model – data mismatch) in case of an ideal network. If we retain all wavelet coefficients that can be described on a 1-degree mesh in the spatial parameterization (4096 coefficients), the reconstruction will be perfect (modulo the model – data mismatch).

Atmospheric inversion could be a way of estimating/verifying self-reported ffCO2 emissions in countries where the uncertainty is high. The uncertainty in emission reports from China is estimated to be 15-20% [Andres et al, 2012], though studies based on the TRACE-P campaign proposed a 54% revision of inventory estimates for 2000 [Suntharalingam et al, 2004] (it was officially revised upwards by 23% between 2006-2007). Other countries have larger variations. These uncertainties affect inventories, but do not affect our inversion method (see paragraph 1). Even if our variable of interest were to be total emissions over a region (nation or province), estimating a spatially variable emission field before spatially aggregating it reduces the aggregation error. However in order to do this, a measurement infrastructure designed with ffCO2 in mind is a requirement. Its size will be determined by whether we are interested estimating total national emissions or we seek fine scale details.

In addition, as mentioned above, our method can be used with other tracers provided we have a spatial parameterization for them.

The introduction section in our paper does not describe the idealized nature of our tests or the limits/caveats on the conclusions that can be drawn from them. It also does not describe the reasoning behind the metrics that were adopted for evaluating our algorithm. We will add them in the revised paper. [Pg7:26 – Pg9:25; Pg29:13 – 24]

Detailed comments

Issue # 1: Then reviewer states "The summary of section 2 states that "mutual incoherence may offer analytical in- sight into the quality of observations and uniqueness of solutions". But in the text, I could not find a proof of this point. It would be very useful for the community if the authors could add examples to illustrate how this method can detect bad quality observations, and show the uniqueness of flux solutions."

We have expressed ourselves badly. What we meant was "mutual incoherence may provide an analytical metric for the quality of observations and consequently, solutions". We will change the sentence in the updated manuscript. [Pg14:26 - 2]

It was not our intention to provide proofs that show low mutual coherence (incoherence) leads to informative observations and is a necessary condition for obtaining a unique solution (without the use of prior information). Necessary conditions for a unique solution also involve a property called Restricted Isometry. Proofs on the necessary conditions for accurate sparse reconstruction can be found in the literature on compressive sensing.

We have, however, calculated the mutual coherence between our transport matrix ("sensing matrix" in compressive sensing terms) and our bases and shown them to be far inferior to the ones achieved in compressive sensing. This is primarily due to where the measurement towers are placed (the network was designed with an eye towards biospheric CO2 fluxes, not ffCO2). Given the lower information content in our observations, the conventional compressive sensing way of solving the inverse problem (i.e., without prior information, except sparsity of representation using wavelets) provided poor estimates (Approach A). We did not investigate the non-uniqueness of solutions.

Note that mutual coherence does NOT help us identify "bad quality" observations in the sense that interference from an anomalous source or a faulty instrument corrupts them.

Instead it helps us identify if the measurement towers "intercept" ffCO2 emissions transported by the wind and thus gather information on them. Given a network of measurement towers and a transport model, mutual coherence provides a metric for the quality of the observations that the network could offer without any noise in the measurements. Noise reduces the quality of the observations further.

Issue # 2: The reviewer states "The purpose of the proposed method is to estimate fossil fuel CO2 emissions. As stated in the conclusion, the fossil fuel CO2 emission is not the only type of emission in nature. I would like to see an example of estimating fossil fuel emissions with this method in the presence of inaccurate biosphere fluxes. It is possible that this method could not work over the entire year, but could possibly work in some months of the year (e.g., January). The authors could then discuss the challenges of estimating fossil fuel emissions in a more realistic scenario."

We thank the reviewer for this suggestion; it provides us with a better structure for explaining what we did, and what remains to be done. The aim of the paper, as described in "Overall response" is to present an inversion algorithm, for rough emission fields, that is insensitive to over/under-estimation in prior beliefs regarding the emissions in question. Performing a real-data inversion, using uncertain biospheric fluxes, would be outside the scope of this paper.

References

[Andres et al, 2012] R. J. Andres et al, "A synthesis of carbon dioxide emissions from fossil-fuel combustion", Biogeosciences, 9, 1845-1871, 2012. doi: 10.5194/bg-9-1845-2012.

[Donoho et al, 2013] D. Donoho et al, "Sparse solutions of underdetermined linear equations by Stagewise Orthogonal Matching Pursuit", IEEE Transactions on Information Theory, 58, 1094-1121, 2012.

[Ray et al, 2014] J. Ray et al, "A multiresolution spatial parameterization for the estimation of fossil-fuel carbon dioxide emissions via atmospheric inversions", Geoscientific Model Development, Geosci. Model Dev., 7, 1901-1918, 2014. doi:10.5194/gmd-7-1901-2014.

[Shiga et al, 2014] Y. P. Shiga et al, "Detecting fossil fuel emissions patterns from sub-continental regions using North American in-situ CO2 measurements", Geophysical Research Letters, 41(12):4381-4388, 2014.

[Suntharalingam et al, 2004] P. Suntharalingam et al, "Improved quantification of Chinese carbon fluxes using CO2/CO correlations in Asian outflows", Journal of Geophysical Research, 109, D18S18, 2004. doi:10.1029/2003JD004362.

Response to reviewers

A sparse reconstruction method for the estimation of multiresolution emission fields via atmospheric inversion

Ray, Lee, Yadav, Lefantzi, Michalak and van Bloemen Waanders, GMDD 7:5623-5659, 2014.

Response to Reviewer No. 3

We thank the reviewer for his/her suggestions and comments. Our responses to his/her suggestions are below.

Overall response: At the very outset we would like to clarify that our study is focused on investigating the algorithmic aspects of a sparse reconstruction method (based on Stagewise Orthogonal Matching Pursuit, StOMP) for estimating rough emission fields, such as that of fossil-fuel CO2 (ffCO2). A sparse reconstruction method is necessary since the spatial parameterization for rough fields tends to be high dimensional (many parameters). The parameters that can be estimated depend on the information content of the observation data, which can change with time/season. The method is not customized to a particular tracer, measurement network or a transport model. Customization to a tracer occurs when we choose a spatial parameterization (a wavelet-based random field model in this study) for use with our sparse reconstruction method. It also occurs when we choose an observational dataset. The method can accommodate prior information on the field being estimated, but only uses its spatial pattern; thus, by design, it is insensitive to under/overestimation of the emissions in the prior information.

The paper investigates which formulations of the inverse problem do and do not work, and explains why. It develops a metric (mutual coherence) to quantify the information content in the observations collected by our measurement network. It finds the information content lacking, which motivates the need to introduce prior information into the inverse problem. We then identify a way to do so; the obvious/intuitive ways do not work. We also show how a wavelet-based field model, designed for modeling fields in rectangular geometries, can be used to estimate emission fields in an irregular region $\mathcal{R}$ (the Lower 48 states of the US). Finally, we show how StOMP can be extended to enforce non-negativity on the estimates. Sparse reconstruction methods are typically not used in atmospheric inversions.

Our motivation to develop this method arose from a need to construct and/or validate gridded inventories of ffCO2. Fortunately, many gridded ffCO2 inventories are available and a wavelet-based spatial parameterization also exists. We demonstrated the method in an idealized, synthetic-data inversion. The idealizations include: (1) assuming ffCO2 to be a radiocarbon-like tracer and ignoring interference by biospheric CO2 which can make ffCO2 estimation impossible except in winter (see Shiga et al., [2014]); (2) using a model-data mismatch ε that is smaller than the one used in real-data inversions and (3) assuming the same distribution for ε for all towers (i.e., ignoring transport model errors). These idealizations allowed us to explore issues related to the algorithm and formulations in a relatively "clean" setting. We also use an observational dataset collected from a

measurement network that was sited with biospheric CO2 fluxes, not ffCO2, in mind (the towers are usually far from locations with high ffCO2 emissions); a network for ffCO2 does not currently exist.

Due to these idealizations adopted in our test, we do not claim that the method can be used to estimate ffCO2 emissions fields in a realistic setting using measurement techniques and infrastructure that are currently available (or could be in the near future). At the very least, our method has to be extended to include the estimation of biospheric fluxes as well as larger and tower-dependent model – data mismatches. This is a substantial body of work and outside the scope of this study. In order to check how accurate the estimates would be, we would have to conduct an OSSE (Observational System Simulation Experiment) or design an ideal network. Our tests also provide no information on the best method to collect information on estimation of ffCO2 emissions over regional scales (tower, airplane transects etc.).

We check our inversion method using the following metrics:

1. As part of our algorithmic development, we modify StOMP to incorporate prior information to improve estimates. We check whether it indeed does so, since the information content of the observations are found to be poor.
2. The aim of sparse reconstruction is to estimate parameters that are supported by data (usually large spatial patterns in the emission field) and remove the details that are not. We check whether this "sparsification" characteristic of the algorithm is still present after including prior information.
3. Our method restricts emission fields in an irregular region $\mathcal{R}$ (while using a wavelet-based model); this incurs a computational cost that can be limited by a user-defined setting. We check if the behavior of the algorithm provides a principled way of computing that setting (e.g., if improvement of results shows a "diminishing returns" behavior with the computational cost).

Note that in this study we do not use the accuracy of the estimated emission fields as a metric for evaluating our inversion method. This is because accuracy of estimation is determined primarily by two factors (once we have specified a model – data mismatch): (1) the suitability of the spatial parameterization for the rough fields being estimated and (2) the information content of the observational dataset. In our previous paper [Ray et al, 2014] we fixed the observational data and used the accuracy of the emission estimates to gauge the quality of the spatial parameterization. The converse procedure – fixing the spatial parameterization and varying the quantity of observational data – is not a very useful direction for investigation, for our StOMP-based method, because of the following reasons:

1. The estimation accuracy of StOMP, as the quantity of observational data is varied, has been investigated in Donoho et al, [2012]
2. If the aim is to obtain a very accurate reconstruction of the ffCO2 field (when we have full discretion to design an ideal observation network/technique), then we are limited only by what the spatial parameterization can capture. As reported in our previous paper [Ray et al, 2014], the spatial parameterization with 1023 wavelet coefficients (parameters) has a relative error of 10% at the 1-degree resolution; this would be recovered (modulo the small model – data mismatch) in case of an ideal network. If we retain all wavelet coefficients that can be described on a 1-degree mesh in the spatial parameterization (4096 coefficients), the reconstruction will be perfect (modulo the model – data mismatch).

Atmospheric inversion could be a way of estimating/verifying self-reported ffCO2 emissions in countries where the uncertainty is high. The uncertainty in emission reports from China is estimated to be 15-20% [Andres et al, 2012], though studies based on the TRACE-P campaign proposed a 54% revision of inventory estimates for 2000 [Suntharalingam et al, 2004] (it was officially revised upwards by 23% between 2006-2007). Other countries have larger variations. These uncertainties affect inventories, but do not affect our inversion method (see paragraph 1). Even if our variable of interest were to be total emissions over a region (nation or province), estimating a spatially variable emission field before spatially aggregating it reduces the aggregation error. However in order to do this, a measurement infrastructure designed with ffCO2 in mind is a requirement. Its size will be determined by whether we are interested estimating total national emissions or we seek fine scale details.

In addition, as mentioned above, our method can be used with other tracers provided we have a spatial parameterization for them.

The introduction section in our paper does not describe the idealized nature of our tests or the limits/caveats on the conclusions that can be drawn from them. It also does not describe the reasoning behind the metrics that were adopted for evaluating our algorithm. We will add them in the revised paper. [Pg7:26 – Pg9:25; Pg29:13 – 24]

General comments

1. The reviewer states (Para 2) "However, it is a big pity to me that the authors did not choose a good test case to prove the practicability of the method developed. As also pointed out by another RC, the setup for their synthetic fossil fuel CO2 (ffCO2) emission inverse problem is too far from the reality. Because of that, I had a difficulty in discussing the feasibility of this method in a fossil fuel emission estimate. In my opinion, what the authors supported by the synthetic experiment is the replication of "non-negative emission fields" in a linear inverse problem, not ffCO2 emission fields. Thus, I would suggest to rework on the synthetic experiment and/or reword some of the text in the manuscript depending on what the authors would like to claim by this manuscript. In the following two sections, I'm trying to discuss several major concerns. Initially, I was listing points I wanted to discuss, but I learned that most of them have been raised by RCs for the author's previous paper (Ray et al. 2014).

http://www.geosci-model-dev-discuss.net/7/1277/2014/gmdd-7-1277-2014-AR1.pdf (last access: Nov 20, 2014)

*So I decided to make use of the *pdf as a reference. I understand that the *pdf was for discussions for Ray et al. (2014), but I think this is still fair to do as in anyways I would raise the exactly same questions/concerns and we probably don't want to replicate the same conversations presented in the *pdf."*

The aim of the paper was to present a sparse reconstruction method for estimating rough emission fields. We demonstrated it on an idealized test case, as described in the "Overall response" above. It is a methodological first step towards estimating ffCO2 emissions in a realistic scenario. There are limits to the conclusions that can be drawn from the idealized test, regarding the usefulness of the method in estimating ffCO2 emissions using existing measurement infrastructure. These were not mentioned in the paper, and we will correct this shortcoming, as described in the "Overall response" above.

Section called "ffCO2 does not seem to be the best emission to be used for the synthetic study"

2. The reviewer states, in para 1, "As acknowledged in Ray et al. (2014), ffCO2 emissions is very difficult to estimate given the existing observation network and also data collected there. The recent paper Shiga et al. (2014) (I see two of the authors are listed) also confirmed that as well. Shiga et al. (2014) also pointed out that the winter month have a better luck in estimating (detecting) ffCO2, but it would be very difficult the rest of the month. Probably this is something the authors should acknowledge in the manuscript."

We agree that we should have cited Shiga et al., [2014], about the limits of estimating ffCO2 emissions. See "Overall response" above for details.

3. The reviewer states, at the end of paragraph 1, "I also strongly feel that the authors need to convince us of the use of tower CO2 for ffCO2 estimation. Or since it was a synthetics study, the authors could come up with an ideal tower network for a ffCO2 emission inverse problem."

We agree with the reviewer that the tower network used in this study will not result in very accurate ffCO2 emission estimates. As described in the "Overall response" above, we use these not-very-informative measurements to uncover numerical characteristics of our method.

The term "ideal tower network" above introduces an ambiguity. If the term means that one is allowed to have as many towers as needed, then the test is not very useful (see "Overall response"). If, on the other hand, the term implies a network with M towers ideally sited for ffCO2 measurement, then one needs to perform a network design first, which in turn requires an ability to solve the (emission estimation) inverse problem, the topic of our paper. Demonstrating the algorithm inside a network optimization loop is outside the scope of the paper.

4. The reviewer points out, in the beginning of paragraph 2, "As we see in the manuscript, the use of existing tower network made the synthetic inversion setup far off from the reality. For example, the error assigned to the radiocarbon-like tracer was 0.1 ppm. This is too small compared to an actual C14 case as pointed out by the review discussion for Ray et al. (2014). It was acknowledged in Ray et al. (2014), but this small error was used again in this manuscript without any note."

This was an oversight. We will update the manuscript to reflect our reason for such a small value of ε. The reason is the same as it was in Ray et al., [2014]– it isolates the effect of the spatial parameterization and the inversion algorithm on the estimates. [Pg8:5 – 16]

5. The reviewer states, in the middle of paragraph 2, "The authors mentioned the use of Carbon Monoxide (CO) in their response to defend the use of the 0.1 ppm error. I would not say no, but it is not clear to me how CO data from the existing tower data would help us to estimate ffCO2 emissions that well. If the authors meant to say the use of satellite-driven CO, that would become another problem as an inversion setup needs to be modified (also, data number would dramatically increase). My point here is that it is very questionable that such an ideal tower-based observational data become available sometime in near future, although I definitely think we push forward to make that happen as a community (in my opinion). The reality is we

don't see any plan to expand the tower network to look at fossil fuel emissions (as far as I know). Perhaps I would be a little bit more convinced if the authors would have used observation from Orbiting Carbon Observatory 2 (OCO2) and/or Greenhouse Gases Observing Satellite (GOSAT) (although I don't know how to derive ffCO2 contribution in XCO2 data)."

We agree that there does not seem to be any movement to design a network for ffCO2 and such low errors are not currently possible. However, these were idealizations that we adopted to demonstrate that we could estimate rough/multiresolution fields, and to isolate the effects of the algorithm and the spatial model on the estimated emissions. We do not claim that the method can be used with the current measurement infrastructure or transport models.

6. The reviewer points, in the last third of paragraph 2, "Also, the emission imposed by Vulcan does not keep the nature of fossil fuel emission fields because of the simplification (averaging). Fossil fuel emissions are not constant over 8 days. We do sometime estimate monthly and/or weekly natural fluxes via inversion, but we do usually have diurnal cycle in forward modeling. Because of points I made above, I thought this manuscript is misleading when I read the abstract saying "We demonstrate the method on the estimation of ffCO2 emissions".

We agree that we have approximated the true emissions (Vulcan) by averaging over 8-day periods. We will update our manuscript to state that the method is demonstrated on an idealized ffCO2 estimation problem. ([Pg8:5 – 16])We will also state the idealizations upfront. We will also point out in the paragraph where we describe how the observations are generated that the averaging over 8 days removes the diurnal variation on ffCO2 emissions. [Pg 22, top 3 lines]

7. The reviewer states, in paragraph 3, "I would suggest to the authors to choose a different application to design a synthetic inversion. It is fair to claim that this manuscript is focusing on a method development. But the synthetic experiment needs to be reasonably close to the reality, especially if a particular target is assumed. If the authors want to stick to the ffCO2 inverse problem, the authors should design more realistic experiment, prove the feasibility of the method and show the reproducibility of the truth. Maybe one thing the authors easily could do is to reword "fossil fuel emissions" to "non- negative emission fields". After proving the reproducibility of the true field, the authors could discuss a possible application to fossil fuel emission estimation (like people do when they propose a numerical scheme). This correction should be fair enough to support the development of the inversion scheme for multi-resolution fields in a linear inverse problem."

Our paper is an algorithmic one, with an idealized test case of estimating ffCO2 emissions. We will reword the paper to use non-negative emission fields where we can. However, the test case, no matter how idealized, is connected to ffCO2 since we use Vulcan, EDGAR and a spatial parameterization for ffCO2. Consequently, we have retained the use of ffCO2, rather than the unwieldy "non-negative emission fields" when describing the results in Sec. 4.

In the Conclusions section, we will discuss the advances that need to be made in order to enable the use of our method in a real-data inversion. [Pg29:13 – Pg30:24]

In the section named "What is the real utility of this method in ffCO2 study"?

8. The reviewer states, in lines 1-9 "Apart from the synthetic study presented for a moment, I would like to discuss about the utility of the method presented in the manuscript (which I thought a major weakness of this manuscript). Again, I understand this manuscript is trying to advance the methodological aspect of future ffCO2 estimation method using atmospheric measurements (which I think it is great). I'm grad to see the authors mentioned current issues in ffCO2 inventory/modeling. But I was a little bit disappointed because this work is not really responsive to those issues. For instance, even in the highly-idealized condition, the method does not give an accurate answer. Given by the nature of the method, this method could only offer a good approximate of ffCO2 fields, but not an accurate field. I thought this is a critical shortcoming."

The aim of the paper was to present a sparse reconstruction method for estimating rough emission fields such as ffCO2. The idealized test case that we employed presents limits on the conclusions that can be drawn from it; we will update our manuscript to reflect them (see "Overall response" above). Also, reconstruction accuracy, when we have full discretion to design the measurement network in our idealized test case, is not a useful metric for judging our method (see "Overall response" and Response no. 3 above).

9. The reviewer states, in lines 9-13, "The authors claimed that the error in their estimation is around 5%. But the 5% is not the same thing as 5% two sigma uncertainty for reported national emissions. In real world, we need to deal with ffCO2 that has diurnal cycle while other strong signals from biosphere are present (and often we have a difficulty in decent angle them)."

The reviewer does not specify where in the text we state 5% as the estimation error. The only instance that we can find is on Pg 5646, line 15. The error is evaluated using the output from Stage I of our algorithm, which computes ffCO2 fluxes *before* non-negativity enforcement. It is also not globally aggregated over $\mathcal{R}$ (the figure stated is root mean square relative error of the 1-degree flux field with respect to Vulcan); the 3-5% error margin that the reviewer states is the uncertainty in total emissions reported by the US. We believe that the comparison is being made between two different things.

On a broader note, we fail to understand why the estimation accuracy of a guessed flux field, before non-negativity enforcement, should matter, especially in such an idealized inversion test case. We have computed and plotted reconstruction errors (after non-negativity enforcement!) in Fig. 2, and they do vary between 2-15%, but only to discriminate between inversion formulations. Nowhere do we claim that the reconstruction errors obtained in our idealized test case are indicative of what could be achieved in a realistic setting.

10. The reviewer states, in lines 13-26, "In addition, the method is assuming a 1x1 degree field where we still don't resolve most of sectoral emission activities (at this spatial resolution, emission spatial proxy such as population and nightlights works pretty well). If I need a ffCO2 emission field, say for this year 2013 for US at a 1x1 degree, I would just project Vulcan emission data (or CDIAC 1x1 degree map) using fuel consumption data (I see this is essentially a very, very crude version (also w/o observation) of what the authors have done in this manuscript). In this way, I don't get any update on the emission spatial extent, but at least I could expect a very good estimate of the annual total emission. Given that, I'm not clear about what the method presented in this manuscript could offer to us. It seems to me that it is very difficult to expect the method to yield a very accurate emission field or update inventories. What we ultimately expect is to be able to tell the discrepancy between what is reported (or

calculated) and what is measured using atmospheric observation (e.g. MRV). But it is not clear to me if the method could offer the opportunity, as it seems to be difficult for atmosphere to tell a subtle difference in emissions especially at an aggregated 1x1 degree. Of course these do not need to be fully addressed, but I would be very curious how the authors envision to approach to the goal from where we are. I think these kind of discussion should be done to figure out what we really need to do, prior to getting into the technical details."

The reviewer's method for updating inventories is applicable when one has an accurate inventory to start with and good fuel usage statistics. As we point out in the "Overall response", there are many large ffCO2 emitters with significant uncertainties in their national-level emission. They are better targets for atmospheric inversion (though, unfortunately, their tower networks are even sparser than the one in North America, and are also not sited with ffCO2 in mind).

We are surprised by the reviewer's statement: "*But it is not clear to me if the method could offer the opportunity as it seems to be difficult for atmosphere to tell a subtle difference in emissions especially at an aggregated 1x1 degree"* - we have performed no tests whatsoever in our paper that investigate how large a change in an inventory we can detect using atmospheric inversion. The magnitude of the change that we could detect would be conditional on the observational dataset that we are provided.

11. The reviewer states, on line 31, "I thought the authors could easily work on more simple inverse problem for non-negative fields using an ideal observation network (and/or satellites) to estimate accurate emissions. I would thus suggest to rework the text and the synthetic experiment to be more responsive to ffCO2 issues if the authors would like to address a ffCO2 issues."

We did consider using a simplified inverse problem. In order to demonstrate that our method could identify and remove a large number of parameters from an emission field model and restrict emissions to an irregular region $\mathcal{R}$, the problem had to be about estimating a 2D field (for a 1D field, these are trivial).

We first considered a simplified 2D problem, with a tower network that would allow us to estimate most of the parameters of the emission field model, and generate accurate solutions. However, in such a data-rich/informative setting, the impact of including the prior would be very muted (Approaches A and C would give very similar solutions). Such a test would not allow us to verify whether our modification of StOMP, to include prior information, had been performed correctly and was contributing information to the inversion (the prior information would be overwhelmed by the observations). Thus we could test only two out of the three features of our new algorithm (non-negativity and restricting emissions in $\mathcal{R}$ and not inclusion of prior information).

Consequently, we adopted a 2D problem where the observations were somewhat informative about the emission field, but still allowed the prior information to be reflected in the solution of the inverse problem. However, we retained some simplifications – no interference by biospheric CO2 fluxes, as well as a small and (statistically) similar model-data mismatch at the towers. Further, the reconstruction errors have a known lower bound (see "Overall response").

12. P5624, L13: The reviewer states "This synthetic inversion was implemented in the highly-idealized synthetic world. Although the Vulcan data was used to create a truth field, this synthetic study is not fair enough to support the implementation of a fossil fuel emission estimation (see my general comment). This needs to be rephrased. Otherwise this could easily give an wrong impression to the audience of GMD."

We agree that the idealized test case imposes limits/caveats on the conclusions that can be drawn from it. We will update the manuscript to make it clear. [Pg29:12 – Pg30:24]. See "Overall response" above.

13. P5624, L17: The reviewer states, "This is certainly an improvement achieved by this paper. But in my opinion, if the authors meant to develop a method to estimate FFCO2, the first thing the authors should try is to get an accurate emission estimate. Even if a method is very computationally heavy, people would be happy to use it to get an accurate estimate. As a study for FFCO2 estimation, this is not very appealing (at least, to me)." He/she states this in the context of our 10x reduction in the computational time needed to enforce emissions in an irregularly shaped region.

We agree with the referee that accuracy is of paramount importance. But our novelty is in Step 1 that essentially generates an imperfect "guess" of the emission field; it does not affect the accuracy of the final estimates. The novelty reduces the time our algorithm spends to generate the guess. Generating the guess quickly has some practical benefits e.g., being able to scale up to large problems. It would be remiss of us not to point out this feature, especially in an algorithmic paper.

14. P5625, L16: The reviewer states "I think the important thing here is how accurate the estimate is." The context is as follows: We describe that spatial parameterizations (or models) of emission fields have too many independent parameters to be estimated from the available atmospheric observations, and thus have to be simplified. Our method performs the simplification based on the observations, and if the information content of the observations varies in time, our method can construct models with variable complexity.

We agree with the reviewer that inversion accuracy should be the guiding principle. Given an observational dataset, the best accuracy is obtained when (1) the spatial parameterization is sufficiently low dimensional to not overfit the observations and (2) sufficiently high dimensional to capture all the structures in the emission field being estimated that are supported by the data. This optimal dimensionality is not known, *a priori,* and our sparse reconstruction method is one way to efficiently identify it, simplify the spatial parameterization and fit it to data in one integrated mathematical formulation.

15. Pg 5626, L11: The reviewer states "I don't see the method developed here is going towards this goal.", the goal being developing spatially resolved estimates of ffCO2 emissions.

We beg to differ with the reviewer's comment that the method we have described is irrelevant to the estimation of ffCO2 emission fields; see "Overall response" above. The arguments that the reviewer has presented show that the current measurement network, along with current transport models and measurement methodologies (inaccurate and expensive radiocarbon observations) will not allow the estimation of ffCO2 emissions fields, but we do not claim that we could do so.

16. P5626, L21: The reviewer states "Since this method is based on the parameterization, it would be difficult to achieve an emission estimate that is accurate enough to updated or improve an emission inventory. This limitation needs to be acknowledged."

We agree. We will update our manuscript with this caveat, at the end of the paragraph. [Pg5:10-14; Pg29:10—13]

17. P5626, L26: The reviewer states "It is unclear to me how this method could offer a method to give an accurate emission estimate using atmospheric measurements." He/she states this in the context of our discussion where we say that satellite and airplane transect do not offer a scalable way of updating inventories.

See Response no. 15 above.

18. Pg 5627, L19: The reviewer states "I would like to learn the benefit this method could offer as opposed to the use of an gridded inventory plus fuel statistics (see my general comment)." He/she makes this remark in the context of our statement that "inventories being updated can serve as very informative priors and reconstruction methods could profitably use them".

The reviewer's method for updating inventories is applicable when one has an accurate inventory to start with and good fuel usage statistics. As we point out in the "Overall response", there are many large ffCO2 emitters with significant uncertainties in their national-level emission. They may be better targets for atmospheric inversion, though unfortunately, their networks are even sparser than in North America, and also were not sited with ffCO2 in mind. Further, atmospheric inversions can also uncover uncertainties in inventories; see Brioude et al., [2012].

19. Pg 5628, L20: The reviewer asks "So here, the authors assumed that biosphere fluxes is perfect? Or ffCO2 can be solved as a separate problem?"

In our idealized test case, we have assumed that ffCO2 can be solved as a separate problem.

20. Pg 5630 L11 and L20: The reviewer states "How would you specify Q here?" (Line 11, Q being the prior covariance). He/she also asks "Given the use of ***f - fpr,*** *would you be able to "correct" an inventory using atmospheric observation?"*

We assume that the reviewer means whether we could correct an inventory given the use of (**f – fpr**) in Eq. 1, since **f** would be affected by under-reporting in the inventory **fpr** unless there was overwhelming atmospheric evidence against it.

We are a little confused by the reviewer's comment, since it implies that we solve Eq. 1 to obtain our emissions estimates. We do *not*. Eq. 1 is based on a multiGaussian assumption (alternatively, a Gaussian random field) for the field being estimated, and we clearly state L18-L23 that this model is not very convenient for expressing rough emission fields like those seen for ffCO2. Consequently we do not define Q, nor do we use (f – fpr) in our inversion. Instead, we use a multiscale random field model developed in our previous paper, which is sufficiently flexible to accommodate rough fields such as ffCO2 emissions.

Our inversion scheme is described in Sec. 3.2 "Posing and solving the inverse problem". It is quite different from Eq. 1. It is the sparse reconstruction method that we have developed in this paper.

21. Pg 5640, L1: The reviewer states "The synthetic observation is really a key in this study. This should be fully described. It is really misleading because CO2 concentration is actually a radiocarbon-like tracer, not normal CO2 concentration usually measured."

We understand the reviewer wants us to make it clear, upfront, that this is a synthetic data study, with all the simplifications and idealizations that have been adopted.

We agree. We will state clearly in the Introduction that the paper develops a method for estimating rough, non-negative emission fields and is tested with an *idealized, synthetic-data* study. [Pg7:26 —Pg8:16; Pg4:27—29]ffCO2 estimation is merely the test case, and we will use a multiscale random field model that was developed for rough ffCO2 emission fields in a previous paper.

22. Pg 5640, L2: The reviewer states "Vulcan is averaged. This should be considered when you evaluate the numerical accuracy. I assume the authors did it right, but I was actually not very sure of it by this manuscript."

Yes, we average Vulcan up to 1 degree resolution in space and 8-days in time. We use this averaged Vulcan as our "truth" emissions, and use it to generate the observational data.

23. Pg. 5640, L7: The reviewer states "Again, this CO2 is a synthetic radiocarbon-like tracer."

We understand that the reviewer wants us to make clear that ffCO2 behaves as a synthetic radiocarbon-like tracer.

We agree. We will explicitly state so. [Pg8:1-4]

24. Pg. 5640, L7: The link to Ray et al, 2013 is dead

We will specify an alternate website from where the technical report can be downloaded.

25. Pg5640, L22 The reviewer asks "So your "truth" is a 8-day averaged Vulcan. Correct? Did you use the averaged Vulcan for creating synthetic CO2 data or hourly Vulcan data? I want to make sure."

We used the 8-day-averaged Vulcan emissions to generate observations. It is our "truth" emission field. The text on L25 is badly phrased and we will make it clear. [Pg22:22 - 24]

26. Pg 5640, L24: The reviewer states, "So the afternoon selection is not applied". This statement is made in the context where we discuss how we obtain the sensitivity of 3-hourly concentration observations to 8-day-averaged emissions by summing up 3-hourly sensitivities

Correct. We use all the observations, and not just the afternoon data.

27. Pg 5641, L2: The reviewer states "This is too small. Also, no transport uncertainties?" He/she states this in the context of the data – model mismatch that we use (0.1 ppmv).

We agree that the model –data mismatch is too small to be realistic. This issue was also raised in our previous paper, and we provide the same explanation.

The primary problem with using a realistic value of ε (1 ppmv rather than 0.1 ppmv) is the placement of the measurement towers – they are far from the sources of ffCO2 emissions leading to measurements that are around 2 ppmv. Adding a noise with variance of 1 ppmv makes them unusable. A true test of our method, in realistic conditions, would require a sensor network sited with ffCO2 emissions in mind. Consequently, we have chosen an idealized scenario and focused on the algorithmic aspects of the problem.

We did mention in the paper that we chose ε to be 0.1 ppmv to construct an idealized scenario within which we could test the quality of the proposed numerical scheme. We will update the manuscript to be more explicit about the reason why. [Pg 8:5 – 16; Pg22:26—28]

28. Pg 5645, L3 The reviewer states "Spell out BAO and MAP. I assume they are not used for the synthetic inversion. Correct? Why were those two sites selected? I saw this in a pessimistic way as the model is showing almost perfect fit to the observation while the emission estimate is still not perfect."

Thank you for catching this error. BAO = Boulder Atmospheric Observatory, Colorado; MAP = Mary's Peak, Oregon. We will update our manuscript with this information. [Pg26:25-26]

BAO and MAP are not being used as a measure of the accuracy of the inverse problem (as an out-of-sample test). They were used in the estimation of the emission field. In Sec 4.3, we check that the algorithm satisfies some of the necessary conditions: (1) after estimation, the emission field should be able to closely approximate the observations and (2) since the measurements are too un-informative to estimate all the parameters in the spatial model for the emission field, the sparse reconstruction method should be able to identify the "un-estimate-able" ones and set them to zero. In Fig. 5, we show that these necessary conditions are met.

The reviewer is correct in remarking that we seem to reproduce observations well, but the estimated emission field is far from the truth (Fig. 2 and 3). This is a consequence of the roughness of the emission field and the fact that measurement sensors are very sensitive to emissions in their vicinity. The spatial model allows rough fields (within limits) that can accommodate localized sources (i.e., set some wavelet coefficients in the spatial model to non-zero values) in the vicinity of the measurement tower. This feature of rough emission fields can be used to match observations very well, if the improvement in the match overcomes the penalty that the sparse reconstruction imposes due to the consequent increase in the complexity of the spatial model. This often happens if the surrounding towers are too far away, or upstream in the wind direction, to provide a constraining influence on what may be an erroneous emission source. The spatial parameterization can also be leveraged to prevent the introduction of such localized sources and consequently requires careful design. This was discussed in our previous paper. Note that if the emission fields are smooth and modeled as multiGaussian fields, such localized sources in the vicinity of the tower cannot be accommodated i.e., in the absence of informative observations, the spatial model imposes a much tighter constraint than our multiscale random field model.

The accuracy of the inversion is thus very dependent on the spatial model and consequently inversion accuracy was discussed in our previous paper. There, we quantified the inversion accuracy entirely in terms of the estimated emission field. Since inverse problems can support non-unique solutions, we use the ability to closely reproduce tower observations as a necessary condition, but not a proxy, for estimation accuracy. We will update our manuscript to (1) clarify that the accuracy of the inversion should be judged using Fig. 2 and 3, as well as the results in the previous paper and (2) Fig. 5 should be seen as a means of verifying that certain necessary conditions that the sparse reconstruction scheme should meet are actually being satisfied. [Pg9:7 – 25]

We will also change the title of the section to "Numerical consistency and computational efficiency". It is a better description of the results presented there.

29. Pg. 5645, L1: The reviewer states "Again, I think the accuracy of estimation needs to be discussed first if ffCO2 emission estimation is the ultimate target of this project."

The reviewer makes this statement at the beginning of a section titled "Numerical accuracy and computational efficiency. While we agree that accuracy of estimation should be the guiding principle, we are a little confused by what he/she implies.

- If the reviewer wants us to discuss the accuracy of the emission fields estimated using our idealized tests, then see Ray et al., [2014], "Overall response" above which explains the reason for them being in our previous paper and Response no. 28.
- If the reviewer wants us to discuss the implications of these results on the accuracy of a real-data inversion, see "Overall response".
- If the reviewer wants us to discuss the accuracy that our method could achieve using M optimally sited towers, see Response no. 3 above.

30. Pg 5645, L13: The reviewer states "The authors should defend that why those small minor feature can be ignored while a very high accuracy is required to improve and/or update inventories."

The use of "unimportant" was a poor choice of words and we will remove it.

What we meant was that in the test case (and real life), the measurement network is unlikely to be sufficiently dense to estimate all the fine scale details of the emission field via atmospheric inversions, and it is better to remove them lest they fit themselves to noise in the data. In our case, we leverage the explicit separation of scales in the multiscale random field model to set these details to zero and simplify the emission model, if doing so does not decrease the quality of the model fit below a threshold. This discrimination is performed in our sparse reconstruction method.

31. Pg 5645, L28: The reviewer states "We should not have a trade off especially in this highly-idealized world. Again, we need an accurate estimate to address an issue in ffCO2 study." This is said in the context of the trade-off between computational efficiency (M_{cs}) and estimated fluxes ($\mathcal{F}_{\mathcal{R}}$ and $\mathcal{F}_{\mathcal{R}}$) in an idealized computation.

As clearly mentioned in the same paragraph, the choice of M_{cs} only affects Step 1, where we develop an approximation of the emission field. The approximation is an "emission" field that is mostly, but not exclusively, non-negative, and is mostly limited to the region $\mathcal{R}$

where non-negative emissions are desired. These emissions are referred to using f_k or $\mathcal{F}$. The approximated "emission" field is processed in Step II of our algorithm to enforce non-negativity; we refer to the non-negative emissions as E. In both steps, we iteratively update the $\mathcal{F}$ or E field to minimize the difference between tower observations and model predictions.

Setting M_{cs} to small number results in a poor approximation and a large number of iterations in Step II. A large M_{cs} spends a long time in Step I, but Step II is quick. The algorithm converges and stops when a certain accuracy metric is met in Step II; the estimated emission field's accuracy is independent of the quality of the approximation that is introduced into Step II via M_{cs}. However, the computational time is not.

We found that increasing M_{cs} (and computational cost) quickly reached a point of diminishing returns, with respect to the quality of the guess that was introduced into Step II. That provided us with a principled way of limiting the time spent in generating a guess.

32. Pg 5646, L15: The reviewer states "This means the method doesn't get both national total and spatial distribution right." This is said in the context of the guesses of emissions being prepared in Step I, prior to non-negativity imposition in Step II.

The reviewer is correct that the guesses of emissions prepared in Step I, and before non-negativity enforcement in Step II, do not get the national total and spatial distribution correctly.

33. Pg. 5647, L16. The reviewer states "Again, this needs to be rephrased." This is said in the context of our statement "we have demonstrated our method on the estimation of ffCO2 emissions ..."

We agree. We have demonstrated estimation of non-negative, spatially rough emissions, in an idealized setting.

34. Pg. 5648, L9: The reviewer states "Two drawbacks are acknowledged in Ray et al. (2014) (See P1917, 1: Need for a good fossil fuel tracer, 2: uncertainty as also mentioned here), but the first one is not acknowledged."

We agree. We will make this correction. [Pg29:13— Pg30:24]

35. Pg 5649, the reviewer points out we misspelt Candés

Fixed.

36. Pg 5652, L2: The reviewer points out a dead link

Fixed.

37. Pg. 5655, Fig 2. The reviewer states "Compared to Table 2 from Asefi-Najafabady et al. (2014), the correlation is not very good. The FFDAS (Nightlight+Population) scores a correlation of 0.86. This is a part of the reason I don't see a utility of this method. Especially this is a synthetic study, the author should seek the way to get much better score." This is said

in the context of two bottom-up inventories, FFDAS v2 and Vulcan, having a very good agreement (spatial correlation) between themselves, far better than the agreement between Vulcan and our inverse problem solution.

Vulcan and FFDAS share many of the underlying data sources. Both FFDAS and Vulcan use the same self-reported emissions and similar data on population density etc. Further, as the authors in [Asefi-Najafabady et al, 2014] clearly point out, the high spatial correlation is due to the presence of pointwise power plant emissions – "FFDASv2 and Vulcan have nearly identical power plant emission data, and the total correlation is driven by the near-perfect agreement for this sector". It is not surprising that the two inventories match so well.

We fail to understand why the reviewer thinks that the agreement between the two is a good way of setting performance/quality thresholds for a technique that would provide an independent check on such inventories.

[Andres et al, 2012] R. J. Andres et al, "A synthesis of carbon dioxide emissions from fossil-fuel combustion", Biogeosciences, 9, 1845-1871, 2012. doi: 10.5194/bg-9-1845-2012.

[Asefi-Najafbady et al, 2014] S. Asefi-Najafbady et al, "A multiyear, global gridded fossil fuel CO2 emission data product: Evaluation and analysis of results", Journal of Geophysical Research: Atmospheres, doi:10.1002/2013JD021296, 2014.

[Brioude et al, 2012] J. Brioude, et al, "A new inversion method to calculate emission inventories without a prior at mesoscale: Application to the anthropogenic CO2 emission from Houston, Texas", Journal of Geophysical Research, 117, D05312, doi:10.1029/2011jD016918, 2012.

[Donoho et al, 2013] D. Donoho et al, "Sparse solutions of underdetermined linear equations by Stagewise Orthogonal Matching Pursuit", IEEE Transactions on Information Theory, 58, 1094-1121, 2012.

[Ray et al, 2014] J. Ray et al, "A multiresolution spatial parameterization for the estimation of fossil-fuel carbon dioxide emissions via atmospheric inversions", Geoscientific Model Development, Geosci. Model Dev., 7, 1901-1918, 2014. doi:10.5194/gmd-7-1901-2014.

[Shiga et al, 2014] Y. P. Shiga et al, "Detecting fossil fuel emissions patterns from sub-continental regions using North American in-situ CO2 measurements", Geophysical Research Letters, 41(12):4381-4388, 2014.

[Suntharalingam et al, 2004] P. Suntharalingam et al, "Improved quantification of Chinese carbon fluxes using CO2/CO correlations in Asian outflows", Journal of Geophysical Research, 109, D18S18, 2004. doi:10.1029/2003JD004362.

Manuscript prepared for Geosci. Model Dev. Discuss.
with version 2014/05/30 6.91 Copernicus papers of the LaTeX class copernicus.cls.
Date: 6 March 2015

A sparse reconstruction method for the estimation of multiresolution emission fields via atmospheric inversion

J. Ray[1], J. Lee[1], V. Yadav[2], S. Lefantzi[1], A. M. Michalak[2], and B. van Bloemen Waanders[3]

[1]Sandia National Laboratories, P.O. Box 969, Livermore, CA, 94551
[2]Carnegie Institution for Science, Stanford, CA, 94305, USA
[3]Sandia National Laboratories, P.O. Box 5800, Albuquerque, NM, 87185-0751, USA

Correspondence to: J. Ray (jairay@sandia.gov)

Abstract

~~We present a sparse reconstruction scheme that can also be used to ensure non-negativity when fitting~~ Atmospheric inversions are frequently used to estimate fluxes of atmospheric greenhouse gases (e.g. biospheric CO_2 flux fields) at the Earth surface. These inversions typically assume that flux departures from a prior model are spatially smoothly varying, which are then modeled using a multivariate Gaussian. When the field being estimated is spatially rough, multivariate Gaussian models are difficult to construct and a wavelet-based ~~random field models to limited observations in non-rectangular geometries.The method is relevant when multiresolution fieldsare estimated using linear inverse problems. Examples include the estimation of emission fields for many anthropogenic pollutants using atmospheric inversion or hydraulic conductivity in aquifers from flow measurements. The scheme~~ field model may be more suitable. Unfortunately, such models are very high-dimensional and are most conveniently used when the estimation method can simultaneously perform data-driven model simplification (removal of model parameters that cannot be reliably estimated) and fitting. Such sparse reconstruction methods are typically not used in atmospheric inversions. In this work, we devise one, and illustrate it in an idealized atmospheric inversion problem for the estimation of fossil-fuel CO_2 ($ffCO_2$) emissions in the lower 48 states of the US.

Our new method is based on ~~three new developments. Firstly, we extend an existing sparse reconstruction method,~~ Stagewise Orthogonal Matching Pursuit (StOMP), ~~to~~ a method used to reconstruct compressively sensed images. Our adaptations bestow three properties to the sparse reconstruction procedure which are useful in atmospheric inversions. We have modified StOMP to incorporate prior information on the ~~target field . Secondly, we develop an iterative method that uses StOMP to impose~~ emission field being estimated and to enforce non-negativity on the estimated field. Finally, ~~we devise a method, based on compressive sensing, to limit the estimated field within an irregularly shaped domain.~~

~~We demonstrate the method on~~ though based on wavelets, our method allows the estimation of ~~fossil-fuel () emissions in the lower 48 states of the US.The application uses a~~ fields in non-rectangular geometries e.g., emission fields inside geographical and political boundaries.

Our idealized inversions use a recently developed multiresolution (i.e., wavelet-based) random field model developed for $ffCO_2$ emissions and synthetic observations of $ffCO_2$ concentrations from a limited set of measurement sites. We find that our method for limiting the estimated field within an irregularly shaped region is about a factor of 10 faster than conventional approaches. It also reduces the overall computational cost by a factor of two. Further, the sparse reconstruction scheme imposes non-negativity without introducing strong nonlinearities, such as those introduced by employing log-transformed fields, and thus reaps the benefits of simplicity and computational speed that are characteristic of linear inverse problems.

1 Introduction

The estimation of spatially-resolved fields e.g., permeability fields in aquifers or CO_2 fluxes in the biosphere, from limited observations, are required for many scientific or engineering analyses. These fields are generally represented on a grid whose spatial resolution is dictated by the analyses. The observations are usually too scarce to allow the estimation of the field's values in each grid-cell independently. If the field is known to be smooth, one can impose a spatial correlation between the grid-cells (e.g., model the field as a realization from a -stationary multivariate Gaussian distribution) and reduce the "effective dimensionality" of the estimation problem so that the limited observations suffice. In contrast, if the field is complex i.e., non-smooth or non-stationary (in the statistical sense, implying different characteristic length-scales at different locations), multivariate Gaussian models are difficult to construct and an alternative parameterization ~~is required~~may be preferable. The parameterization has to be low-dimensional i.e., have few independent parameters, so that they can be estimated from limited observations.

The construction of the spatial parameterization for complex fields poses a stiff challenge. The parameterization is usually problem-dependent and sometimes based on heuristics. One may use an easily observed covariate (or predictor) of the field being estimated to construct such a model; for example, see Ray et al. (2014) for a description on how images of lights at night were used to create a spatial parameterization for fossil-fuel CO_2 ($ffCO_2$) emissions. However, one is never quite sure if the resultant parameterization is too simple or too complex

. In – in the former case, the estimates will be needlessly inaccurate. In , while in the latter case, one may not obtain a unique solution or the estimates may reproduce the noise in the observations (overfitting). Further, Consequently, one uses some method, for example, AIC (Akaike Information Criterion), to devise models of suitable complexity. However, if the quality of the observations changes with time, then, ideally, a different parameterization is required has to be constructed for each time instant. In practice, often the simplest model that can be used with all the observations is employed. This degrades estimation accuracy.

Sparse reconstruction methods can allow one to circumvent these problem which arise from the dimensionality of spatial parameterization (also called the random field model). Sparse reconstruction methods such as Matching Pursuit (MP; Mallat and Zhang, 1993), Orthogonal Matching Pursuit (OMP; Tropp and Gilbert, 2007) and Stagewise OMP (StOMP; Donoho et al., 2012) are optimization methods that are used to fit high-dimensional models to limited observations. Unlike other optimization methods, these methods enforce sparsity i.e., they identify the model parameters that are not informed by the observations and set them to zero. This is accomplished by augmenting the objective function (usually a ℓ_2 norm of the data - model discrepancy or residuals) with a penalty formulated as a ℓ_1 norm over the parameters being estimated. The parameters (The ℓ_2 norm of a vector $\mathbf{x}$ is defined as $||\mathbf{x}||_2 = \sqrt{\sum_i x_i^2}$, while the ℓ_1 norm is $||\mathbf{x}||_1 = \sum_i |x_i|$.) An optimizer is used to manipulate model parameters to minimize the objective function. The parameters that do not impact the residual appreciably are quickly driven to zero to minimize , as it minimizes the ℓ_1 penalty . This i.e., the optimizer performs dimensionality reduction while it fits the model to data. This "model simplification" characteristic of sparse reconstruction methods allows one to dispense with the offline construction of a spatial parameterization and postulate a general, high-dimensional random field model instead; thereafter, the optimization method simplifies (reduce the dimensionality of) the random field model in a data-driven manner. In case of observations with time-variant quality, sparse reconstruction methods have the potential to be particularly useful.

Our interest in sparse reconstruction methods arises from a need to develop accurate spatially-resolved estimates of estimates of emissions that are not smoothly distributed in space. ffCO$_2$ emissions . These estimates are one such example. Estimates of ffCO$_2$ emissions are used to

assess regional contributions to greenhouse gas emissions and to drive climate change simulations (Andres et al., 2012). Currently, spatially-resolved estimates of $ffCO_2$ emissions are typically derived from national-level emissions inventories, and are mapped spatially using population density or some other proxy of human activity; examples of such spatially-resolved inventories are described in Gurney et al. (2009); Olivier et al. (2005); Rayner et al. (2010); Oda and Maksyutov (2011). Their shortcomings arise from errors in national/provincial reporting and the choice of the proxy used in spatial disaggregation (Andres et al., 2012). Recently, the possibility of using atmospheric observations to constrain fossil fuel emissions, and thereby improve inventories, has been explored (Pacala et al., 2010). Such applications involve the solution of an inverse problem driven by $ffCO_2$ concentration measurements (Rayner et al., 2010). Note that such improvements would be contingent on a good representation of estimation problem within the context of an inversion, including the use of a suitable parameterization for the emissions, the characterization of transport model errors, and the availability of an observational network that is sufficient to provide an adequate constraint on $ffCO_2$ emissions. $ffCO_2$ emissions for individual urban domes have been estimated using atmospheric measurements (Turnbull et al., 2011; McKain et al., 2012; Kort et al., 2012) i.e., without solving an inverse problem, but existing methods do not offer a scalable approach to updating entire inventories in this manner.

As a step towards enabling such applications, we constructed a wavelet-based spatial parameterization, called the Multiscale Random Field (MsRF; Ray et al., 2014), to represent $ffCO_2$ emission fields. The MsRF was used to model $ffCO_2$ emissions in the lower 48 states of the US at $1^\circ \times 1^\circ$ spatial resolution. ~~It~~ The MsRF covers a rectangular region described by the corners $(24.5^\circ N, 63.5^\circ W)$ and $(87.5^\circ N, 126.5^\circ W)$. The emissions are modeled using Haar wavelets, which provide the sparsest representation of $ffCO_2$ emissions in the relevant region. The model has $O(10^3)$ independent model parameters ~~, and due~~ which were selected using images of lights at night. Due to its high dimensionality, the MsRF model cannot be used directly given realistic in situ observational limitations. However, a data-driven dimensionality reduction of the MsRF model, using a sparse reconstruction method, could help ~~to~~ constrain the inverse problem and make it possible to capture coarse spatial patterns of $ffCO_2$ emissions (and, perhaps, finer details in the vicinity of the sensors), conditioned on atmospheric measurements.

The use of sparse reconstruction methods poses certain methodological challenges. Firstly, these reconstruction methods do not provide a mechanism for imposing non-negativity, which is a requirement when estimating ~~fields like emissions~~emission fields. Secondly, sparse reconstruction methods have, to date, been used with wavelet-based random field models which can only model rectangular domains; in contrast, the geometry of ~~emission fields are~~ emission fields could be decided by geographical or political boundaries. (A random field model is a spatial parameterization for a field defined on a grid. It can be constructed using orthogonal bases such as wavelets; the wavelets' weights are the model parameters and are treated as random variables. Realizations of these random variables produce a realization of the field. Depending upon the choice of the basis set e.g., if it contains only a subset of wavelets that can be supported by the grid, the random field model may be able to produce only a subset of the infinite number of fields that the grid can support). Finally, sparse reconstruction methods do not provide a simple mechanism to incorporate prior information or guesses of the field being estimated, a common technique to ensure a unique solution to an inverse problem. This is because methods such as OMP and StOMP were largely developed for the reconstruction of compressively sensed images (Candes and Wakin, 2008) where prior information is weak. In contrast, ~~inventories being updated~~ many emission fields of an anthropogenic nature have inventories that can serve as very informative priors and reconstruction methods could profitably use them.

Our previous work (Ray et al., 2014) focused on ~~a~~the spatial parameterization (the MsRF described above) for estimating ffCO_2 emission fields via atmospheric inversion. In this paper, we describe the methodological innovations in sparse reconstruction techniques that allowed us to perform the inversion, despite the high-dimensionality of the parameterization. These innovations result in an extension of StOMP which can address the peculiarities of reconstructing an emission field. The StOMP extension will be demonstrated in a top-down inversion, using synthetic observations generated from a known, "ground-truth" emission field so that we may examine ~~the accuracy of~~certain algorithmic and numerical aspects of the estimation technique, as described below. The novel algorithmic developments addressed in this paper are:

1. *Incorporation of a prior model of spatially rough emissions: ~~emissions:~~* We demonstrate a novel and simple method to introduce prior information on spatially rough emission

fields (in the form of an approximate field $\boldsymbol{f}_{\text{pr}}$) into StOMP. Currently, sparse reconstruction methods employ no other prior information beyond the phenomenological observation that most fields can be represented quite accurately with a sparse set of judiciously chosen wavelet bases (Candés and Romberg, 2007).

Note, that the term "prior model" or "prior information" is used somewhat loosely here since our method is not strictly Bayesian. However, $\boldsymbol{f}_{\text{pr}}$ serves a similar function by providing regularization in the inverse problem.

2. *Estimating fields in irregularly shaped regions:* The MsRF model, being based on wavelets, can only model fields in rectangular domains, whereas our emission field is distributed over an irregular region $\mathcal{R}$, the lower 48 states of the US. We demonstrate how this geometrical constraint can be imposed efficiently using random projections, a technique that underlies much of compressive sensing. The reconstruction of fields in non-rectangular geometries has no parallel in the compressive sensing of images and the method discussed in this paper is the first of its kind.

3. *Imposition of non-negativity:* The estimation of ~~fluxes (including emissions) is posed~~the emission field is posed as a linear inverse problem (see Sect. 2). Non-negativity of emissions can be enforced by log-transforming the field, but converts the problem into a non-linear one, requiring computationally expensive, iterative sparse reconstruction methods, like the one developed in Li and Jafarpour (2010). We develop a simple, iterative post-processing method to enforce non-negativity on the estimated ffCO_2 emissions. The non-negativity enforcement mechanism uses StOMP but does not use the MsRF model. The imposition of non-negativity in a sparse reconstruction setting has never been been explored before; for example, in Hirst et al. (2013), the non-negativity constraint was not applied to CH_4 emissions from landfills.

In this study, we demonstrate our method on ~~the estimation of~~ an idealized atmospheric inversion of a spatially rough emission field in $\mathcal{R}$. The method is general, but we use ffCO_2 as the test case. The idealizations are enumerated below.

1. We assume that $ffCO_2$ can be measured independently without interference from biospheric CO_2 fluxes. As described in Ray et al. (2014), this could be performed using $\Delta^{14}CO_2$ (radiocarbon) or other non-CO_2 tracers, but the measurement technology is expensive and far from being widely deployable.

2. Inversions require us to adopt a statistical error model for the mismatch between observations and model predictions using the estimated emission field. This error quantifies the aggregate of measurement uncertainties and errors introduced by the approximations in the transport model, among others. It varies between measurement locations. In this study, we model this mismatch as i.i.d. Gaussian random variables. We assume a value for the standard deviation of the distribution that is too small compared to what is possible using existing transport models and measurement technologies; further, we use the same error model for all the measurement locations (details in Sec. 4). The small error allowed us to investigate the numerical aspects of our formulation and solution algorithms without being substantially affected by observational noise. The small error was also required due to the nature of the measurement network employed in the synthetic data test (see below).

The synthetic measurements are obtained at a set of 35 towers, a network that existed in 2008 (see Ray et al. (2013) for their locations). This network, sited with biospheric CO_2 measurements in mind, has towers which tend to be far from urban areas and thus sources of $ffCO_2$ emissions~~in $\mathcal{R}$~~. Consequently the modeled $ffCO_2$ concentrations at these towers tend to be low, forcing us to employ an error model that is unrealistically small. These idealizations lead to limits on the inferences that can be drawn regarding the use of our method in a real-data inversion for $ffCO_2$ emission fields; they are discussed in Sec. 5.

We will estimate the emission field at $1^\circ \times 1^\circ$ resolution. Emission fields are averaged over 8 days, and estimated over 360 days i.e., we estimate $360/8 = 45$ fields. $ffCO_2$ emission from the Vulcan inventory (Version 1) (http://vulcan.project.asu.edu/index.php; Gurney et al., 2009), serve as the "ground-truth", to generate the synthetic or pseudo-observations $\boldsymbol{y}^{\text{obs}}$ of time-variant $ffCO_2$ concentrations. (The Vulcan inventory provides hourly $ffCO_2$ emis-

sions at ~~0.1°~~ 10 kilometer resolution for the lower 48 states of the US for 2002; it can also be downloaded at 0.1° resolution.) The prior model $\boldsymbol{f}_{\text{pr}}$ will be constructed using the Emission Database for Global Atmospheric Research (Source: European Comission, Joint Research Centre (JRC)/Netherlands Environmental Assessment Agency (PBL). Emission Database for Global Atmospheric Research (EDGAR), release version 4.0, http://edgar.jrc.ec.europa.eu, 2009; Olivier et al., 2005), which provides a single emission field at 1° resolution for 2005. These choices were driven solely by the easy availability of data.

~~The paper is~~ We evaluate our inversion method using the following metrics. First, we check whether the incorporation of prior information into our modification of the StOMP algorithm improves estimates. Secondly, we investigate the "sparsifying" nature of our algorithm. The aim of sparse reconstruction is to estimate parameters supported by data (usually large-scale spatial patterns in the rough emission field) and remove details that are not. We check whether this property of StOMP is retained after our modifications. Finally, we check the efficiency with which our method reconstructs emission fields inside an irregular $\mathcal{R}$. Our use of a wavelet-based spatial parameterization incurs a computational cost which can be limited by a user-defined setting. We check if there is a principled way of computing this setting e.g. if improvements in results follow a "diminishing returns" behavior with the computational cost

Note that in this study, we do not use the accuracy of the estimated field as a metric for evaluating our method; we only use estimation accuracy to select between competing formulations of the inverse problem . The estimation accuracy depends on (1) the spatial parameterization (the MsRF) and (2) the information content of the dataset, and was explored in detail in our previous paper (Ray et al., 2014). There, we fixed the observational data and used the accuracy of the estimated emission field to gauge the quality of the MsRF. The converse problem - fixing the MsRF and varying the quantity of data - is not very useful for our StOMP-based algorithm, since StOMP's sensitivity to data was addressed in Donoho et al. (2012).

The paper is structured as follows. In Sect. 2, we review sparse reconstruction techniques, their use with wavelet models of fields and the tenets of compressive sensing that establish the necessary conditions for successful sparse reconstructions. In Sect. 3, we pose the inverse

problem and describe the numerical method used to solve it. Three formulations, differing in the manner in which they incorporate $\boldsymbol{f}_{\text{pr}}$ are examined. In Sect. 4 we perform inversion tests with synthetic data to select the best formulation. We also explain, using the properties required for sparse reconstruction, why the selected formulation performed better than the others. The efficacy of limiting the estimated field within $\mathcal{R}$ using random projections is also investigated. Conclusions are in Sect. 5.

2 Background

In this section, we review techniques used to estimate CO_2 fluxes, compressive sensing, and the use of sparse reconstruction in inverse problems.

Estimation of CO_2 *fluxes:* Let the vector $\boldsymbol{f}$ be the CO_2 flux defined on a grid ~~.~~ with $N_{\mathcal{R}}$ grid cells. Let $\boldsymbol{f}$ be of size $KN_{\mathcal{R}}$, representing a flux field defined over K time-periods. The flux is assumed to be time-invariant during a given time period. The transport of CO_2 is modeled as that of a passive scalar, i.e. the concentration of CO_2 due to $\boldsymbol{f}$ at an arbitrary set of sites, is given by $\boldsymbol{y} = \mathbf{H}\boldsymbol{f}$. Here, $\boldsymbol{y}$ is a vector K_sN_s long, N_s being the number of locations where measurements are collected K_s times over the K time-periods.. The matrix $\mathbf{H}$ ($K_sN_s \times KN_{\mathcal{R}}$) contains the sensitivity of measurements to a CO_2 source in each grid-cell and is computed using an atmospheric transport model such as the Stochastic Time-Inverted Lagrangian Transport Model (STILT; Lin et al., 2003). In an atmospheric inversion, CO_2 concentration $\boldsymbol{y}^{\text{obs}}$ are measured at a limited set of locations, usually a set of measurement towers (as in our case) or as column-averaged satellite soundings. The measurements are too few or too uninformative to estimate $\boldsymbol{f}$, with each grid-cell treated independently. In case of biospheric fluxes, a prior flux $\boldsymbol{f}_{\text{pr}}$ (with the same dimensions as $\boldsymbol{f}$) can be obtained from a biogeochemical process-based model such as CASA (Carnegie-Ames-Stanford Approach; Potter et al., 1993). The discrepancy $(\boldsymbol{f} - \boldsymbol{f}_{\text{pr}})$ is usually modeled as a multivariate Gaussian field with covariance $\mathbf{Q}$, (a $KN_{\mathcal{R}} \times KN_{\mathcal{R}}$ matrix) and the estimation of $\boldsymbol{f}$ is typically performed by minimizing the objec-

tive function

$$J = \underbrace{(\boldsymbol{y}^{\text{obs}} - \mathbf{H}\boldsymbol{f})^T \mathbf{R}_e^{-1} (\boldsymbol{y}^{\text{obs}} - \mathbf{H}\boldsymbol{f})}_{\text{Observation term}} + \underbrace{(\boldsymbol{f} - \boldsymbol{f}_{\text{pr}})^T \mathbf{Q}^{-1} (\boldsymbol{f} - \boldsymbol{f}_{\text{pr}})}_{\text{Prior term}}, \quad (1)$$

where $\mathbf{R}_e$ is a diagonal matrix with the data – model variances and includes many sources of errors including measurement errors, aggregation errors and transport model inaccuracies. Methods to solve this linear inverse problem are reviewed in Ciais et al. (2010). A comparison of biogenic CO_2 fluxes and ffCO_2 emissions (Fig. 1 in Ray et al., 2014) shows that ffCO_2 are multiscale in nature and a multivariate Gaussian field approximation of $(\boldsymbol{f} - \boldsymbol{f}_{\text{pr}})$ is unlikely to be accurate. This motivated us to construct the MsRF model for ffCO_2 emission fields (Ray et al., 2014). The solution of an inverse problem using MsRF requires the use of a sparse reconstruction method that, to date, ~~have been commonly~~ has been used in the reconstruction of compressively sensed images.

Compressive sensing of images: Compressive sensing (Romberg, 2008; Candes and Wakin, 2008) is a very efficient means of representing images using wavelets. Wavelets are a family of orthogonal bases with compact support that are routinely used to model complex fields, including ffCO_2 emissions (Ray et al., 2014). Compact support refers to the fact that a wavelet is defined over a finite region ("compact support"). This is in contrast to other commonly used bases e.g. $\sin(k\pi x), -\infty \leq x \leq \infty, k \in \mathbb{Z}$, which have infinite support. However, like Fourier bases, wavelets are orthogonal; the scalar product of two different wavelets of the same type and order e.g., Daubechies wavelets of order 4, is zero. Compressive sensing (CS) is based on two key tenets: *compressible representation* and *encoding via random projections*. CS assumes that an image, projected onto a suitable wavelet basis set, will yield wavelet weights (represented by a vector $\boldsymbol{w}$) that are mostly very small (i.e., a *compressible* representation) and can be set to zero. Removing the "small" wavelets results in a *sparse* approximation of the image. Encoding via random projections is more involved and determines the necessary conditions for successful sampling. Random encoding is central to our method for applying boundary conditions, viz. limiting ffCO_2 emissions within complex, non-rectangular boundaries.

Consider an image $\mathbf{g}$ of size N, that can be represented sparsely using $L \ll N$ wavelets. Random encoding, as used in CS, asserts that the image may be sampled by projecting it onto a set of random vectors $\boldsymbol{\psi}_j$, to obtain compressive measurements $\mathbf{g}'$, of size N_m, $L < N_m \ll N$:

$$\mathbf{g}' = \boldsymbol{\Psi}\mathbf{g} = \boldsymbol{\Psi}\boldsymbol{\Phi}\boldsymbol{w} = \mathbf{A}\boldsymbol{w}, \tag{2}$$

where the rows of the sampling matrix $\boldsymbol{\Psi}$ consist of the random vectors $\boldsymbol{\psi}_j$, the columns of $\boldsymbol{\Phi}$ consist of the orthonormal basis vectors (the wavelets) $\boldsymbol{\phi}_i$ and $\boldsymbol{w}$ are the weights (or coefficients) of the wavelets. $\boldsymbol{\Phi}$ is a $N \times N$ matrix while $\boldsymbol{\Psi}$ is $N_m \times N$. The bulk of the theory was established in Candes and Tao (2006); Donoho (2006); Candes et al. (2006) and Baraniuk et al. (2008).

In order that one may recover the original image $\mathbf{g}$ from $\mathbf{g}'$ using sparse reconstruction, $\boldsymbol{\Psi}$ and $\boldsymbol{\Phi}$ must satisfy *incoherence* and a *restricted isometry property* (Candes and Wakin, 2008). Incoherence implies that no row ψ_k in $\boldsymbol{\Psi}$ is co-aligned with column ϕ_l in $\boldsymbol{\Phi}$ and thus collects information on all bases. It is ensured by choosing some well known wavelets bases (e.g., Haars, Daubechies 4 and 8 etc.) for $\boldsymbol{\Phi}$ and random vectors for $\boldsymbol{\Psi}$ (Tsaig and Donoho, 2006; Coifman et al., 2001). This is formally quantified by the *mutual coherence* $\mu(\boldsymbol{\Psi}, \boldsymbol{\Phi})$ of $\boldsymbol{\Psi}$ and $\boldsymbol{\Phi}$:

$$\mu(\boldsymbol{\Psi}, \boldsymbol{\Phi}) = \sqrt{N} \max_{1 \le (k,l) \le N} | < \psi_k, \phi_l > | = \sqrt{N} \max(|A_{ijkl}|), \tag{3}$$

where ~~A_{ij}~~ A_{kl} are elements of $\mathbf{A}$. Each row of $\boldsymbol{\Psi}$ is normalized to a unit vector. The term $| < \psi_k, \phi_l > |$ is the projection of row ψ_k on a wavelet basis ϕ_l. Co-alignment of a row $\psi_{k'}$ with a wavelet $\phi_{l'}$ would lead to $A_{k'l'} = 1$ and $A_{k'l} = 0$ for all $l \neq l'$, indicating that a random vector $\psi_{k'}$ collects information on only one wavelet. The scaling by $\sqrt{N}$ is conventional. A small mutual coherence ~~(i.e., incoherence of $\boldsymbol{\Psi}$ and $\boldsymbol{\Phi}$)~~ ensures that all projections of $\boldsymbol{\Phi}$ on the rows of $\boldsymbol{\Psi}$ are of moderate magnitude ($\mathrm{O}(10^{-1}) - \mathrm{O}(10^{-3})$). A small mutual coherence aids accurate reconstruction. When $\mu(\boldsymbol{\Psi}, \boldsymbol{\Phi}) \ll \sqrt{N}$, we loosely refer to $\boldsymbol{\Psi}$ and $\boldsymbol{\Phi}$ as being incoherent. The restricted isometry property (RIP) is a condition imposed on $\mathbf{A}$ which ensures that $\boldsymbol{w}$ can be recovered from $\mathbf{g}'$ uniquely without the use of priors (except sparsity). We did not pursue this thread since the use of a prior – making the inventory that supplies $\boldsymbol{f}_{\mathrm{pr}}$ consistent with observations – is the motivation behind this investigation.

Sparse reconstruction of images from compressive measurements: The aims of reconstruction in CS are to (1) recover the sparsity pattern (alternatively, identify the components of $\boldsymbol{w}$ that can be estimated from $\mathbf{g}'$) and (2) estimate those elements of $\boldsymbol{w}$ that are informed by $\mathbf{g}'$ while setting the rest to zero. The former can be realized by minimizing the ℓ_0 norm of $\boldsymbol{w}$ while the latter is typically achieved by minimizing the ℓ_2 norm of the measurement - model discrepancy. However, an objective function that contains a ℓ_0 norm is discontinuous, and consequently ℓ_0 is replaced by an ℓ_1 norm, which is more tractable (Donoho et al., 2012). Thus the optimization problem is posed as:

$$\underset{\boldsymbol{w}\in\mathbb{R}^N}{\text{minimize}} \; ||\boldsymbol{w}||_1, \qquad \text{subject to } ||\mathbf{g}' - \mathbf{A}\boldsymbol{w}||_2 < \epsilon_2. \tag{4}$$

This optimization problem can be solved using methods like MP, OMP and StOMP. Bayesian equivalents also exist (Ji et al., 2008; Babacan et al., 2010), where Laplace priors are used to enforce sparseness in the inferred $\boldsymbol{w}$. Algorithms based on convex optimization that serve the same purpose are reviewed in Jafarpour (2013). All these algorithms are general and do not exploit any particular structure in $\mathbf{g}$ except sparsity. However, one may also create a prior model for wavelet distributions e.g., by using a database of similar images, for higher quality reconstructions (Duarte et al., 2005; La and Do, 2005; Baraniuk et al., 2010; He and Carin, 2009). In order to do so, sparse reconstruction methods have to be modified to incorporate prior information.

Sparsity is sometimes used to solve inverse problems in physics, with the $\boldsymbol{\Psi}$ operator representing the physical process. Most of these inverse problems have been in the estimation of log-transformed permeability fields (Li and Jafarpour, 2010; Jafarpour, 2013), seismic tomography (Loris et al., 2007; Simons et al., 2011; Gholami and Siahkoohi, 2010) and estimation of point and distributed emissions (Hirst et al., 2013; Martinez-Camara et al., 2013). A more detailed review of the sparse reconstruction methods can be found in our previous paper (Ray et al., 2014). Most of these inverse problems involved nonlinear models, i.e. $\boldsymbol{y} = \mathbf{a}(\boldsymbol{w})$, rather than $\boldsymbol{y} = \mathbf{A}\boldsymbol{w}$, for which incoherence (and RIP) are not well-defined and consequently were not investigated.

To summarize, sparse reconstruction techniques and wavelet-based random field models have been used in nonlinear inverse problems. In contrast, the problem of ~~flux estimation (both biospheric and fossil-fuel)~~ estimation of spatially rough emission fields is linear, raising the possibilities that (1) the same approach may offer a solution to the emission estimation problem and (2) mutual incoherence may ~~offer analytical insight into~~ provide analytical metrics for the quality of observations and ~~uniqueness of solutions.~~ consequently, solutions. We build on the principles of compressive sensing and sparse reconstruction methods to design an inversion scheme for rough emission fields. In particular, we show (using coherence metrics) why the use of $\boldsymbol{f}_{\text{pr}}$ was necessary. We also show the degree of computational saving achieved when we use random projections to limit ffCO_2 emissions within $\mathcal{R}$.

3 Formulation of the estimation problem

Ray et al. (2014) developed a Multiscale Random Field model (the MsRF model) for ffCO_2 emissions in the US. The MsRF model allows ffCO_2 emissions to be represented as $\boldsymbol{f} = \boldsymbol{\Phi w}$, where $\boldsymbol{\Phi}$ is a collection of Haar wavelets. Consequently, the observational term in Eq. (1) can be written as $||\boldsymbol{y}^{\text{obs}} - \mathbf{H\Phi w}||_2^2$. Comparing with Eq. (2), we see that the transport model $\mathbf{H}$ serves as the sampling matrix $\boldsymbol{\Psi}$. Since we seek to estimate the wavelet weights $\boldsymbol{w}$ from $\boldsymbol{y}^{\text{obs}}$, an optimization problem like Eq. (4) could be posed with the constraint $||\boldsymbol{y}^{\text{obs}} - \mathbf{A}\boldsymbol{w}||_2 < \epsilon_2$, $\mathbf{A} = \mathbf{H\Phi}$. In order to solve this problem via sparse reconstruction, one requires that $\mathbf{H}$ and $\boldsymbol{\Phi}$ be incoherent. As we will show in Sect. 4.2, the incoherence requirement is not met, and sparsity (solely) is not sufficient to solve the problem accurately (as tested in Sect. 4.1). Consequently we modify StOMP to incorporate a prior emission field $\boldsymbol{f}_{\text{pr}}$. We also adapt it to accommodate fields defined over irregularly shaped domains as well as to ensure non-negativity of the estimated field.

Let $\boldsymbol{f}$ be a time-variant, non-negative field defined in an irregular region $\mathcal{R}$, gridded with $N_{\mathcal{R}}$ grid-cells. In our case $\boldsymbol{f}$ models ffCO_2 emission fields. The field is averaged over a time-period T and covers K time-periods, i.e. it is a vector $N_{\mathcal{R}}K$ long. $\boldsymbol{f}$ drives a linear model of

observations of $ffCO_2$ concentrations:

$$\boldsymbol{y}^{\text{obs}} = \boldsymbol{y} + \epsilon = \mathbf{H}\boldsymbol{f} + \epsilon, \tag{5}$$

where $\mathbf{H}$ is the sensitivity matrix obtained from an atmospheric transport model (see Sect. 2), ϵ is the ~~measurement error and~~ model - data mismatch due to measurement and transport model errors and $\boldsymbol{y}^{\text{obs}}$ is a vector of time-variant measurements collected at N_{s} measurement towers. Each tower collects K_{s} measurements over the K time-periods, i.e. $\boldsymbol{y}^{\text{obs}}$ is a vector $K_{\text{s}}N_{\text{s}}$ long. The $\mathbf{H}$ matrix is $(K_{\text{s}}N_{\text{s}}) \times (N_{\mathcal{R}}K)$.

3.1 Prior models

We employ two prior models in our work – the MsRF model for $ffCO_2$ emissions and a time-invariant approximation of $ffCO_2$ emissions $\boldsymbol{f}_{\text{pr}}$. The MsRF is a collection of wavelets and models emissions in the logically rectangular domain given by the corners (24.5° N, 63.5° W) and (87.5° N, 126.5° W). The MsRF discretizes the domain using a dyadic $2^M \times 2^M$ mesh. Haar wavelets are defined on all M levels of this dyadic grid, but not all of them are retained in the MsRF. Wavelets constituting the MsRF model are chosen using radiance-calibrated images of lights at night (http://www.ngdc.noaa.gov/dmsp/download_radcal.html; Cinzano et al., 2000), which serve as a proxy for human activity and thus capture the spatial patterns of $ffCO_2$ emissions. The emission field is allowed to assume non-zero values only within $\mathcal{R}$, the lower 48 states of the US. We denote the field during the kth time-period as $\boldsymbol{f}_k$ and model it as

$$\boldsymbol{f}_k = w'_k\phi' + \sum_{s=1}^{M}\sum_{i,j} w_{s,i,j,k}\phi_{s,i,j}, \quad \{s,i,j\} \in W^{(s)} = \boldsymbol{\Phi}\boldsymbol{w}_k. \tag{6}$$

where $W^{(s)}$ contains the L wavelets that constitute the MsRF model. L is a fraction of the 4^M wavelets that can be supported by a $2^M \times 2^M$ mesh.

The MsRF is also the starting point for developing the second prior model $\boldsymbol{f}_{\text{pr}}$. The MsRF provides a sparse representation of the radiances $\mathbf{X}^{(s)}$:

$$\mathbf{X}^{(s)} = w'_{(X)}\phi' + \sum_{l,i,j} w_{(X),s,l,i,j}\phi_{l,i,j}, \{l,i,j\} \in W^{(s)}. \tag{7}$$

(8)

$\mathbf{X}^{(s)}$ is used to calculate a time-invariant prior model for ffCO$_2$ emissions as $\boldsymbol{f}_{\text{pr}} = c\mathbf{X}^{(s)}$. c is computed such that

$$\int_{\mathcal{R}} \overline{\boldsymbol{f}_V} \mathrm{d}A = \int_{\mathcal{R}} \boldsymbol{f}_{\text{pr}} \mathrm{d}A = c \int_{\mathcal{R}} \mathbf{X}^{(s)} \mathrm{d}A = c \int_{\mathcal{R}} \left(w'_{(X)}\phi' + \sum_{l,i,j} w_{(X),s,i,j}\phi_{l,i,j} \right) \mathrm{d}A, \{l,i,j\} \in W^{(s)}. \tag{9}$$

Equation (9) implies that c is calculated such that both $\overline{\boldsymbol{f}_V}$ and $\boldsymbol{f}_{\text{pr}}$ provide the same value for the total emissions in $\mathcal{R}$. $\overline{\boldsymbol{f}_V}$ in our case is the annually-averaged 2005 emission field obtained from EDGAR. The leftmost term $\int_{\mathcal{R}} \overline{\boldsymbol{f}_V} \mathrm{d}A$ quantifies the total emissions as predicted by EDGAR over $\mathcal{R}$. The term $c\int_{\mathcal{R}} \mathbf{X}^{(s)} \mathrm{d}A$ is an estimate of emissions over the same region but modeled using $\boldsymbol{f}_{\text{pr}}$. The rightmost term simply replaces $\mathbf{X}^{(s)}$ with its wavelet model, per Eq. 8. The details of how the MsRF and $\boldsymbol{f}_{\text{pr}}$ were constructed are in Ray et al. (2014). $\boldsymbol{f}_{\text{pr}}$ differs from the "ground-truth" (Vulcan emissions aggregated over the lower 48 states) by 5–25 % (see Fig. 9 in Ray et al., 2014).

3.2 Posing and solving the inverse problem

We seek emissions over an entire year (360 days), i.e., we seek ~~$\mathbf{F} = \{\boldsymbol{f}_1, \boldsymbol{f}_2, \ldots \boldsymbol{f}_K\} = \{\boldsymbol{\Phi w}_1, \boldsymbol{\Phi w}_2, \ldots \boldsymbol{\Phi w}_K\} = \tilde{\boldsymbol{\Phi}}\boldsymbol{w}$. F~~

$\boldsymbol{F} = \{\boldsymbol{f}_1, \boldsymbol{f}_2, \ldots \boldsymbol{f}_K\} = \{\boldsymbol{\Phi w}_1, \boldsymbol{\Phi w}_2, \ldots \boldsymbol{\Phi w}_K\} = \tilde{\boldsymbol{\Phi}} \boldsymbol{w}$. $\boldsymbol{F}$ models the field in $\mathcal{R} \cup \mathcal{R}'$, where $\mathcal{R}'$ models the region outside $\mathcal{R}$ (but inside the rectangular domain modeled by the MsRF) with zero $ffCO_2$ emissions. We separate out the fluxes in $\mathcal{R}$ and $\mathcal{R}'$ by permuting the rows of $\tilde{\boldsymbol{\Phi}}$

$$\mathbf{F}\boldsymbol{F} = \begin{pmatrix} \mathbf{F}_{\mathcal{R}} \boldsymbol{F}_{\mathcal{R}} \\ \mathbf{F}_{\mathcal{R}'} \boldsymbol{F}_{\mathcal{R}'} \end{pmatrix} = \begin{pmatrix} \tilde{\boldsymbol{\Phi}}_{\mathcal{R}} \\ \tilde{\boldsymbol{\Phi}}_{\mathcal{R}'} \end{pmatrix} \boldsymbol{w},$$

where $\tilde{\boldsymbol{\Phi}}_{\mathcal{R}}$ and $\tilde{\boldsymbol{\Phi}}_{\mathcal{R}'}$ are $(N_{\mathcal{R}} K) \times (LK)$ and $(N_{\mathcal{R}'} K) \times (LK)$ matrices, respectively. Here $N_{\mathcal{R}'}$ is the number of grid-cells in $\mathcal{R}'$. The modeled concentrations at the measurement towers, caused by $\mathbf{F}_{\mathcal{R}} \boldsymbol{F}_{\mathcal{R}}$, can be written as ~~$\boldsymbol{y} = \mathbf{H}\mathbf{F}_{\mathcal{R}} \boldsymbol{y} = \mathbf{H}\boldsymbol{F}_{\mathcal{R}}$~~. For arbitrary $\boldsymbol{w}$, ~~$\mathbf{F}_{\mathcal{R}'} \boldsymbol{F}_{\mathcal{R}'}$~~ (the emissions in $\mathcal{R}'$) are not zero and ~~$\mathbf{F}_{\mathcal{R}'} = 0$~~ $\boldsymbol{F}_{\mathcal{R}'} = 0$ will have to be imposed as a constraint in the inverse problem.

Specifying the constraint in individual grid-cells is not very efficient since it leads to $N_{\mathcal{R}'} K$ constraints. This can get very large in a global inversion at high spatial resolutions. Instead, we adapt an approach from compressive sensing to enforce this constraint approximately. Consider a $M_{\text{cs}} \times (N_{\mathcal{R}'} K)$ matrix $\mathbf{R}$, whose rows are direction cosines of random points on the surface of $N_{\mathcal{R}'} K$-dimensional unit sphere. This matrix is called a uniform spherical ensemble (Tsaig and Donoho, 2006). The M_{cs} projections of the emission field ~~$\mathbf{F}_{\mathcal{R}'} \boldsymbol{F}_{\mathcal{R}'}$~~ on $\mathbf{R}$ i.e., ~~$\mathbf{R}\mathbf{F}_{\mathcal{R}'}$ compressively samples $\mathbf{F}_{\mathcal{R}'}$~~ $\mathbf{R}\boldsymbol{F}_{\mathcal{R}'}$ compressively samples $\boldsymbol{F}_{\mathcal{R}'}$ and setting them to zero during inversion allows us to enforce zero emissions outside $\mathcal{R}$. In Sect. 4.3, we will investigate the degree of computational saving afforded by imposing the ~~$\mathbf{F}_{\mathcal{R}'} = 0$~~ $\boldsymbol{F}_{\mathcal{R}'} = 0$ constraint in this manner. The problem is now modeled as:

$$\mathbf{Y}\boldsymbol{Y} = \begin{pmatrix} \boldsymbol{y}^{\text{obs}} \\ 0 \end{pmatrix} \approx \begin{pmatrix} \mathbf{H}\,\tilde{\boldsymbol{\Phi}}_{\mathcal{R}} \\ \mathbf{R}\,\tilde{\boldsymbol{\Phi}}_{\mathcal{R}'} \end{pmatrix} \boldsymbol{w} = \mathbf{G}\boldsymbol{w}. \tag{10}$$

In this equation, $\mathbf{G}$ is akin to $\mathbf{A}$ in Eq. (2). The left hand side ~~$\mathbf{Y}$~~ $\boldsymbol{Y}$ is approximately equal to $\mathbf{G}\boldsymbol{w}$ since the observations $\boldsymbol{y}^{\text{obs}}$ contain measurement errors that cannot be modeled with $\mathbf{H}$.

The case where ~~$\mathcal{R}'$~~ $\mathcal{R}'$ contains non-zero emissions requires the use of boundary fluxes and is discussed in Ray et al. (2014).

The wavelet coefficients $\boldsymbol{w}$ in Eq. (10) are not normalized and usually display a large range of magnitudes. The wavelets in $W^{(s)}$ at finer scales, i.e. those with a small support, tend to have coefficients with a large magnitude. Their small support cause the fine-scale wavelets to impact only neighboring measurement towers. In contrast, wavelets at the coarser scales have large "footprints" that span multiple measurement locations. Total emissions in $\mathcal{R}$, as well as $\boldsymbol{y}^{\text{obs}}$, are very sensitive to their coefficients. Solving Eq. (10) as-is incorporates no information from $\boldsymbol{f}_{\text{pr}}$ beyond the selection of wavelets to be included in $\tilde{\boldsymbol{\Phi}}$. We explore the incorporation of $\boldsymbol{f}_{\text{pr}}$ in the estimation of $\boldsymbol{w}$ using three different approaches:

Approach A: This is the baseline approach and solves Eq. (10) as-is. The lack of normalization of $\boldsymbol{w}$, in conjunction with the sparse reconstruction procedure described below, leads to artifacts that will be described in Sect. 4.1.

Approach B: In this formulation, we include $\boldsymbol{f}_{\text{pr}}$ as a "prior". We write the emissions as ~~$\mathbf{F} = \boldsymbol{f}_{\text{pr}} + \Delta\mathbf{F}$~~ $\boldsymbol{F} = \boldsymbol{f}_{\text{pr}} + \Delta\boldsymbol{F}$. Substituting into Eq. (10), we get ~~$\mathbf{Y} \approx \mathbf{H}\boldsymbol{f}_{\text{pr}} + \mathbf{G}\Delta\boldsymbol{w}$~~ $\boldsymbol{Y} \approx \mathbf{H}\boldsymbol{f}_{\text{pr}} + \mathbf{G}\Delta\boldsymbol{w}$, where $\Delta\boldsymbol{w} = \boldsymbol{w} - \boldsymbol{w}_{(X)}$. Here, $\boldsymbol{w}_{(X)} = c\{w'_{(X)}, w_{(X),s,i,j}\}$, $\{s,i,j\} \in W^{(s)}$, where c is obtained from Eq. (9). Simplifying, we get

$$\Delta\boldsymbol{Y}\boldsymbol{Y} = \boldsymbol{Y}\boldsymbol{Y} - \mathbf{H}\boldsymbol{f}_{\text{pr}} \approx \mathbf{G}\Delta\boldsymbol{w}, \tag{11}$$

Approach C: ~~The incorporation of the spatial patterns in~~ In Approach B we expressed the true flux $\boldsymbol{F}$ as an additive correction over $\boldsymbol{f}_{\text{pr}}$ ~~into the estimation procedure can be performed in an alternative manner. We note that~~, thus incorporating the prior information in $\boldsymbol{f}_{\text{pr}}$. In Approach C, we use the spatial pattern of $\boldsymbol{f}_{\text{pr}}$, as captured by its wavelet coefficients $\boldsymbol{w}_{(X)}$ ~~can be used~~, to normalize $\boldsymbol{w}$. We rewrite Eq. (10) as

$$\boldsymbol{Y}\boldsymbol{Y} \approx \mathbf{G}\,\text{diag}(\boldsymbol{w}_{(X)})\mathbf{B}\,\text{diag}(\mathbf{B}^{-1}\boldsymbol{w}_{(X)}^{-1}) = \mathbf{G}'\boldsymbol{w}' = \begin{pmatrix} \mathbf{H}\,\tilde{\boldsymbol{\Phi}}'_{\mathcal{R}} \\ \mathbf{R}\,\tilde{\boldsymbol{\Phi}}'_{\mathcal{R}'} \end{pmatrix} \boldsymbol{w}', \; \mathbf{B} = c\,\text{diag}(\boldsymbol{w}_{(X)}), \tag{12}$$

where $\boldsymbol{w}' = \{w_{s,i,j}/(c\,w_{(X),s,i,j})\}, \{s,i,j\} \in W^{(s)}$ ~~is the normalized set of wavelet coefficients~~ are the wavelet coefficients normalized by those of $\boldsymbol{f}_{\text{pr}}$, $\tilde{\boldsymbol{\Phi}}'_{\mathcal{R}} = \tilde{\boldsymbol{\Phi}}_{\mathcal{R}}\,\text{diag}(\boldsymbol{w}_{(X)})$ and $\tilde{\boldsymbol{\Phi}}'_{\mathcal{R}'} =$

$\tilde{\mathbf{\Phi}}_{\mathcal{R}'}\ \mathrm{diag}(\boldsymbol{w}_{(X)})$. If $\boldsymbol{f}_{\mathrm{pr}}$ is close to $\boldsymbol{F}$, the elements of $\boldsymbol{w}'$ will be O(1). If $\boldsymbol{f}_{\mathrm{pr}}$ is a gross underestimate, the elements of $\boldsymbol{w}'$ will still be of the same order of magnitude, but not O(1). Thus normalization with $\boldsymbol{w}_{(X)}$ removes the large differences that exist between the wavelet coefficients at different scales.

In all the three cases, we obtain an underdetermined set of linear equations of the form

$$\boldsymbol{\Upsilon} \approx \boldsymbol{\Gamma}\boldsymbol{\zeta}. \tag{13}$$

Here $\boldsymbol{\Upsilon}$ represents $\boldsymbol{Y}$ in Approaches A and C, and $\Delta\boldsymbol{Y}$ in Approach B. $\boldsymbol{\Gamma}$ represents $\mathbf{G}$ in Approaches A and B and $\mathbf{G}'$ in Approach C. $\boldsymbol{\zeta}$ represents $\boldsymbol{w}$ in Approach A, $\Delta\boldsymbol{w}$ in Approach B and $\boldsymbol{w}'$ in Approach C.

Since $\boldsymbol{y}^{\mathrm{obs}}$ is obtained from a set of locations sited with an eye towards biospheric CO_2 fluxes (see Ray et al., 2013) it is unlikely that it will allow the estimation of all the elements of $\boldsymbol{\zeta}$. Further, a priori, we do not know the identity of these "un-estimateable" elements and so we use sparse reconstruction to find and compute them. Equation (13) is recast similar to Eq. (4):

$$\underset{\boldsymbol{\zeta}\in\mathbb{R}^N}{\text{minimize}} \quad ||\boldsymbol{\zeta}||_1, \quad \text{subject to} \quad ||\boldsymbol{\Upsilon} - \boldsymbol{\Gamma}\boldsymbol{\zeta}||_2^2 < \epsilon_2. \tag{14}$$

We solve Eq. (14) using StOMP. $||\boldsymbol{\zeta}||_1$ is minimized by setting as many elements of $\boldsymbol{\zeta}$ to zero as possible, thus enforcing sparsity. Meanwhile, the constraint $||\boldsymbol{\Upsilon} - \boldsymbol{\Gamma}\boldsymbol{\zeta}||_2$ ensures that the solutions being proposed by the optimization procedure provide a good reproduction of the observations. Note $\boldsymbol{\zeta}$ contains only the wavelets in $W^{(s)}$. The StOMP algorithm is detailed in Donoho et al. (2012).

We will refer to this step in the estimation procedure as Step I.

3.3 Enforcing non-negativity on ~~$\mathbf{F}_{\mathcal{R}}$~~ $\boldsymbol{F}_{\mathcal{R}}$

Estimates of $\boldsymbol{w}$ calculated by StOMP do not necessarily provide ~~$\mathbf{F}_{\mathcal{R}} = \tilde{\mathbf{\Phi}}_{\mathcal{R}}\,\boldsymbol{w}$~~ $\boldsymbol{F}_{\mathcal{R}} = \tilde{\mathbf{\Phi}}_{\mathcal{R}}\,\boldsymbol{w}$ that are non-negative. In practice, negative values of ~~$\mathbf{F}_{\mathcal{R}}$~~ $\boldsymbol{F}_{\mathcal{R}}$ occur in only a few grid-cells and are usually small in magnitude. A large fraction of elements of $\boldsymbol{w}$ are set to zero by StOMP.

Having identified the sparsity pattern, i.e., the spatial scales that can be estimated from $\boldsymbol{y}^{\text{obs}}$, we devise an iterative procedure for enforcing non-negativity on ~~$\mathbf{F}_{\mathcal{R}}$~~ $\boldsymbol{F}_{\mathcal{R}}$. We discard ~~$\mathbf{F}_{\mathcal{R}'}$~~ $\boldsymbol{F}_{\mathcal{R}'}$ and manipulate the field (the emissions) in $\mathcal{R}$ directly, rather than via the wavelet coefficients.

We seek the non-negative vector ~~$\mathbf{E} = \{E_i\}, i = 1 \dots Q, Q = (N_{\mathcal{R}} K)$~~ $\boldsymbol{E} = \{E_i\}, i = 1 \dots Q, Q = (N_{\mathcal{R}} K)$ such that

$$\frac{||\boldsymbol{y}^{\text{obs}} - \mathbf{H}\mathbf{E}||_2}{||\boldsymbol{y}^{\text{obs}}||_2} \frac{||\boldsymbol{y}^{\text{obs}} - \mathbf{H}\boldsymbol{E}||_2}{||\boldsymbol{y}^{\text{obs}}||_2} \leq \epsilon_3. \tag{15}$$

~~$\mathbf{E}$~~ $\boldsymbol{E}$ is constructed iteratively through a sequence ~~$\mathbf{E}_1, \mathbf{E}_2, \dots \mathbf{E}_0$~~ $\boldsymbol{E}_1, \boldsymbol{E}_2, \dots \boldsymbol{E}_0$ is initialized by using the absolute values of ~~$\mathbf{F}_{\mathcal{R}}$~~ $\boldsymbol{F}_{\mathcal{R}}$ calculated by solving Eq. (14). At each iteration m, we seek a correction $\xi = \{\xi_i\}, i = 1 \dots Q$, where $|\xi_i| \leq 1$, such that

$$\begin{aligned}
\mathbf{E}\boldsymbol{E}^{(m)} &= \text{diag}(\exp(\xi_1), \exp(\xi_2), \dots, \exp(\xi_Q)) \mathbf{E}\boldsymbol{E}^{(m-1)} \\
&\approx \text{diag}(1 + \xi_1, 1 + \xi_2, \dots, 1 + \xi_Q) \mathbf{E}\boldsymbol{E}^{(m-1)} \\
&= \mathbf{E}\boldsymbol{E}^{(m-1)} + \Delta\mathbf{E}\boldsymbol{E}^{(m-1)}, \text{ where } \Delta\mathbf{E}\boldsymbol{E}^{(m-1)} = \xi^T \mathbf{E}\boldsymbol{E}^{(m-1)}.
\end{aligned}$$

Since the field must satisfy ~~$\boldsymbol{y}^{\text{obs}} \approx \mathbf{H}\mathbf{E}^{(m)}$~~ $\boldsymbol{y}^{\text{obs}} \approx \mathbf{H}\boldsymbol{E}^{(m)}$, we get

$$\boldsymbol{y}^{\text{obs}} - \mathbf{H}\mathbf{E}\boldsymbol{E}^{(m-1)} = \Delta\boldsymbol{y} \approx \mathbf{H}\Delta\mathbf{E}\boldsymbol{E}^{(m-1)} \tag{16}$$

This is an underconstrained problem, and we seek the sparsest set of updates ~~$\Delta\mathbf{E}^{(m-1)}$~~ $\Delta\boldsymbol{E}^{(m-1)}$ using StOMP. The corrections are calculated, and the field updated as

$$\begin{aligned}
\xi_i &= \text{sgn}\left(\frac{\Delta E_i^{(m-1)}}{E_i^{(m)}}\right) \max\left(1, \left|\frac{\Delta E_i^{(m-1)}}{E_i^{(m)}}\right|\right), \\
E_i^{(m)} &= E_i^{(m-1)} \exp(\xi_i),
\end{aligned} \tag{17}$$

to obtain ~~$\mathbf{E}^{(m)}$~~ $\boldsymbol{E}^{(m)}$. The convergence requirement in Eq. (15) is checked with ~~$\mathbf{E}^{(m)}$~~ $\boldsymbol{E}^{(m)}$, and if not met, the iteration count is updated $m := m + 1$ and Eq. (16) is solved again.

We will refer to this step in the estimation procedure as Step II.

4 Numerical results

In this section, we test the sparse estimation technique in Sect. 3, using synthetic observations. The time-period T over which the ffCO$_2$ emissions are averaged is 8 days. $K = 45$, i.e., we estimate emissions over $8 \times 45 = 360$ days. $N_\mathrm{s} = 35$ towers, which are a subset of NOAA's Earth System Research Laboratory (ESRL) Global Monitoring Division's cooperative air sampling network (Tans and Conway, 2005); their locations are in Ray et al. (2013). These towers provide continuous observations of CO_2 concentrations (in parts per million by volume, ppmv), and three-hourly averaged synthetic observations are used here (i.e. $K_\mathrm{s} = 24/3 \times 8 \times 45 = 2880$). We discretize the domain covered by the MsRF using $1^\circ \times 1^\circ$ grid-cells i.e., $M = 6$. The number of grid-cells in the entire domain (the rectangle with the corners (24.5° N, 63.5° W) and (87.5° N, 126.5° W)), N, is $4^M = 4096$, which is also equal to the number of wavelets that can be defined on the mesh. The number of wavelets retained in the MsRF, L, is 1031. $\mathcal{R}$ denotes the lower 48 states of the US. They are covered with $N_\mathcal{R} = 816$ grid-cells. The number of grid-cells outside $\mathcal{R}$, $N_{\mathcal{R}'} = N - N_\mathcal{R} = 3280$.

The $\mathbf{H}$ matrix in Eq. (5) is calculated per the description in Gourdji et al. (2012). We use the Stochastic Time-Inverted Lagrangian Transport Model (Lin et al., 2003), with wind fields from the Weather Research & Forecasting model (Skamarock and Klemp, 2008), version 2.2, driven by 2008 meteorology to compute $\mathbf{H}$. Concentration sensitivities are calculated at 3 h intervals over a North American grid, at a resolution of $1^\circ \times 1^\circ$. The sensitivity of the CO_2 concentration at each observation location due to the flux at each grid-cell is calculated in units of $\mathrm{ppmv\ \mu mol^{-1}\ m^2\ s^1}$. The sensitivity of $\boldsymbol{y}$ to the 8 day averaged emissions were obtained from the 3 h sensitivities by simply adding the $8 \times 24/3 = 64$ sensitivities that span the 8 day period.

The true ffCO$_2$ emissions in $\mathcal{R}$ are obtained, for 2002, from the Vulcan inventory. Hourly Vulcan fluxes are coarsened from 0.1° resolution to 1°, and averaged to 8 day periods. These ~~fluxes~~

8-day averaged fluxes at 1° resolution are multiplied by $\mathbf{H}$ to obtain $ffCO_2$ concentrations at the measurement towers. Note that averaging over 8 days removes the diurnal variations of $ffCO_2$ emissions in Vulcan. Observations are generated every 3 h and span a full year. A measurement error $\epsilon \sim N(0, \sigma^2)$ is added to the concentrations to obtain $\boldsymbol{y}^{\text{obs}}$ (see Eq. 5), as used in Eq. (10). The same σ is used for all towers. We use $\sigma = 0.1$ ppmv, ~~representing an idealized~~ which is too small and represents an idealized inversion scenario that is used here to test the quality of the proposed numerical method. Realistic values of transport model errors for some of the towers used in this study are in Gourdji et al. (2012). Radiocarbon measurement errors can be found in Turnbull et al. (2011).

4.1 Comparison of optimization formulations

We choose between Approaches A, B and C by solving the inverse problem for the $ffCO_2$ emission field. The inversion is performed for the emissions ~~$\mathbf{F} = \{\boldsymbol{f}_k\}, k = 1 \ldots K$~~ $\boldsymbol{F} = \{\boldsymbol{f}_k\}, k = 1 \ldots K$, for the entire year. The following parameters are used in the inversion process: $\epsilon_2 = 10^{-5}, \epsilon_3 = 5.0 \times 10^{-4}, M_{\text{cs}} = 13\,500$ i.e., 300 random projections for each 8 day period. The rationale for these values can be found in our previous paper (Ray et al., 2014).

In Fig. 2 we plot the estimated emissions during the 31st 8 day period, as calculated using Approaches A, B and C. The true emissions are also plotted for reference. Four quadrants are also plotted for easier comparison and reference. The distribution of measurement towers is very uneven, with most of the towers being concentrated in the Northeast quadrant, where we expect the reconstruction to be most accurate. We see that Approach A (Fig. 2, top right) provides estimates that have large areas in the Northwest (NW) and Southwest (SW) quadrants with moderate levels of $ffCO_2$ emissions. In contrast, the true emissions (Fig. 2, top left) are mostly empty. Thus we see that the minimization of $||\boldsymbol{\zeta}||_1$ (alternatively $||\boldsymbol{w}||_1$) drives the wavelet coefficients to small values, but not identically to zero. In Fig. 2 (bottom left), Approach B provides estimates that show much structure in the Eastern quadrants, and the patterns seen in $\boldsymbol{f}_{\text{pr}}$ (see Ray et al., 2014) are reproduced. The reason is as follows. While $\boldsymbol{f}_{\text{pr}}$ captures the broad, coarse scale patterns of $ffCO_2$ emissions, it incurs significant errors at the finer

scales. Equation (11) seeks to rectify the discrepancy between $\boldsymbol{f}_{\text{pr}}$ and true emissions using observations. However, as mentioned in Sect. 3.2, fine-scale wavelets tend to have large wavelet coefficients and the minimization of $||\boldsymbol{\zeta}||_1$ (alternatively $||\Delta \boldsymbol{w}||_1$) removes them since the constraint $||\boldsymbol{\Upsilon} - \boldsymbol{\Gamma}\boldsymbol{\zeta}||_2^2 < \epsilon_2$ is not very sensitive to individual wavelets at the fine scale. (See Gerbig et al. (2009) for a discussion on the largely local impact of a CO_2 flux source.) The inability to rectify the fine-scale discrepancies lead to a final ffCO_2 estimate that resembles $\boldsymbol{f}_{\text{pr}}$ in the finer details. Figure 2 (bottom right) plots the estimates obtained using Approach C, which uses normalized wavelet coefficients $\boldsymbol{w}'$. The estimates from Approach C show large areas of little or no emissions in the Western quadrants, similar to the true emissions in the top left figure. In the Eastern quadrants, the emissions show less spatial structure than the true emissions as well as those obtained using Approach A.

The quality of the estimate is due to both the MsRF model and the new sparse reconstruction scheme. The limited observations are sufficient to allow the estimation of the coarse MsRF wavelets, and in certain areas e.g., the NE quadrant, finer details. The MsRF model is sufficiently flexible to accommodate the spatial heterogeneity in detail, but requires a sparse reconstruction method to address the high dimensionality that such flexibility entails. Further, the multiresolution nature of MsRF model allows the accurate estimation of coarse scale patterns of ffCO_2 emissions i.e., we expect that aggregate measures of emission quality, such as integrated emissions in $\mathcal{R}$, will be accurate. It will incur larger errors as the domain of integration is shrunk.

In Fig. 3 (left) we evaluate the accuracy of the reconstruction quantitatively. We integrate the emissions in $\mathcal{R}$ to obtain the country-level ffCO_2 emissions and compare that with the emissions from Vulcan. We plot a time-series of errors defined as a percentage of total, country-level Vulcan emissions

$$\text{Error}_k\ (\%) = \frac{100}{K}\sum_{k=1}^{K}\frac{E_k - E_{V,k}}{E_{V,k}},\ \text{where}\ E_k = \int_{\mathcal{R}} \underline{\mathbf{E}}\underline{\boldsymbol{E}}_k\,\mathrm{d}A\ \text{and}\ E_{V,k} = \int_{\mathcal{R}} \boldsymbol{f}_{V,k}\mathrm{d}A. \tag{18}$$

Here, $\boldsymbol{f}_{V,k}$ are Vulcan emissions averaged over the kth 8 day period and ~~$\mathbf{E}_k$~~ $\underline{\boldsymbol{E}}_k$ are the non-negativity enforced emission estimates in the same time period. A positive error denotes an

overestimation by the inverse problem. In Fig. 3 (right) we plot the Pearson correlation coefficient between the true and reconstructed emissions in $\mathcal{R}$ over the same duration. We define the Pearson correlation coefficient between ~~$\mathbf{E}_k$~~ $\boldsymbol{E}_k$ and $\boldsymbol{f}_{V,k}$ as

$$C\left(\mathbf{E}\boldsymbol{E}_k, \boldsymbol{f}_{V,k}\right) = \frac{\mathrm{cov}(\mathbf{E}_k, \boldsymbol{f}_{V,k})}{\sigma_{\mathbf{E}_k}\sigma_{\boldsymbol{f}_{V,k}}} \frac{\mathrm{cov}(\boldsymbol{E}_k, \boldsymbol{f}_{V,k})}{\sigma_{\boldsymbol{E}_k}\sigma_{\boldsymbol{f}_{V,k}}},$$

where ~~$\sigma^2_{\mathbf{E}_k}$~~ $\sigma^2_{\boldsymbol{E}_k}$ and $\sigma^2_{\boldsymbol{f}_{V,k}}$ are the variances of the true and reconstructed fluxes and $\mathrm{cov}(Z_1, Z_2)$ is the covariance between two random variables Z_1 and Z_2. It is clear that Approach B provides the worst reconstructions, with the largest errors and smallest correlations. Approach C tends to over-predict emissions a little more than Approach A, but has better spatial correlation with the Vulcan emissions.

In Fig. 4 we see the essential difference between Approach A and C. We plot the reconstruction error (left) and correlation between true and reconstructed emissions (right) in the Northeast (NE) and Northwest (NW) quadrants. Errors in the emissions are represented as a percentage of the total (true) emissions in that quadrant. We see the Approach C has smaller errors in both the quadrants. It also provides higher correlation in the NW quadrant, which does not have many measurement towers (white diamonds in Fig. 2). Both the approaches have errors of opposite signs in the quadrants which largely cancel out when errors are assessed over $\mathcal{R}$ as a whole, leading to approximately similar estimation accuracies by both the approaches in Fig. 3. However, the estimates produced by Approach A (without the use of $\boldsymbol{f}_{\mathrm{pr}}$) show larger spatial variability and error than Approach C. This is because normalization using $\boldsymbol{w}_{(X)}$ and minimization of $||\boldsymbol{\zeta}||_1$ (alternatively $||\boldsymbol{w}'||_1$) prevents large departures from $\boldsymbol{f}_{\mathrm{pr}}$ and also rectifies the tendency to remove large wavelet coefficients belonging to the finer wavelets. Approach C therefore provides a formulation that is more accurate and robust at the quadrant scale, even though both have similar fidelity at the scale of $\mathcal{R}$.

4.2 Evaluating formulation using compressive sensing metrics

Having established empirically that Approach A is less accurate than Approach C, we explain why this is so. We employ coherence metrics for this purpose.

In compressive sensing, random matrices such as Gaussians, Hadamard, Circulant/Toeplitz or functions such as noiselets (Tsaig and Donoho, 2006; Gan et al., 2008; Yin et al., 2010; Tuma and Hurley, 2009) serve as $\mathbf{\Psi}$. In Fig. 5, we plot the distribution of $\log_{10}(|A_{i,j}|)$, the elements of $\mathbf{A}_{\mathbf{\Psi}} = \mathbf{\Psi}\mathbf{\Phi}$ for these "standard" sampling matrices. $\mathbf{\Phi}$ contains only the wavelets in $W^{(s)}$. Note that $\max(|A_{ij}|)$ specifies the mutual coherence and small values of $\max(|A_{ij}|)$ indicate informative measurements. We see that $\log_{10}(|A_{i,j}|)$ may assume continuous (Gaussian and circulant sampling matrices) or discrete (Hadamard, scrambled-block Hadamard and noiselets) distributions, and generally lie between -3 and -1. This provides a range for the level of coherence observed in theoretical CS analyses.

In Eq. (10), $\mathbf{H}$ serves a similar sampling purpose, and the efficiency of sampling depends on the incoherence between $\mathbf{H}$ and $\mathbf{\Phi}$. We construct a new $\mathbf{H}'$ by picking the rows of $\mathbf{H}$ corresponding to 2 towers and for the 21st and 22nd 8 day periods. We compute $\mathbf{A}_{\mathbf{H}'} = \mathbf{H}'\mathbf{\Phi}$, and in Fig. 5, plot the log-transformed magnitudes of the elements of $\mathbf{A}_{\mathbf{H}'}$. The distributions for the two towers are almost identical. We clearly see that, unlike $\mathbf{A}_{\mathbf{\Psi}}$, $\mathbf{A}_{\mathbf{H}'}$ contains a significant number of elements that are close to 1, and a large number of elements that are close to 0 (e.g. near 10^{-6}). This is a consequence of the rows of $\mathbf{H}'$ being approximately aligned to some of the columns of $\mathbf{\Phi}$ and consequently, nearly orthogonal to others. The small values in $\mathbf{A}_{\mathbf{H}'}$ indicate that the CO_2 concentration prediction $\boldsymbol{y}$ at the two selected towers are insensitive to many of the wavelets i.e., to many scales and locations, as observed in Sect. 4.1. Further, the coherence $\mu(H', \mathbf{\Phi})$ is larger than $\mu(\mathbf{\Psi}, \mathbf{\Phi})$, indicating a sampling efficiency a few orders of magnitude inferior to those achieved in the CS of images. Consequently Approach A, based solely on sparsity, and identical to the method adopted in CS, would not work well. Thus, Approach C, which employed both sparsity and $\boldsymbol{f}_{\text{pr}}$, proved superior to Approach A.

4.3 Numerical ~~accuracy~~ consistency and computational efficiency

We now address some of the numerical aspects of the solution. The results presented here are *not* tests of accuracy of the estimated emission field; estimation accuracy also depends on the MsRF and was investigated in Ray et al. (2014). Here we empirically verify that certain necessary conditions of our sparse reconstruction are satisfied.

In Fig. 6 (top) we plot $\boldsymbol{y}$ predicted by the reconstructed emissions at 2 towers, BAO ~~and MAP.~~ (Boulder Atmospheric Observatory and MAP (Mary's Peak, Oregon). These towers were included in the inversion and are *not* being used as an out-of-sample test of the accuracy of the estimated emission field. Rather, the MsRF for rough fields allows the estimation of local sources which can help reproduce a tower's measurements very closely, unless neighboring towers provide a constraint; in a sparse network, this is not always possible. Thus an accurate reproduction of a tower's observations is not necessarily a sign of an accurately estimated emission field, but a bad reproduction can be a sign of a malfunctioning sparse reconstruction method. We see that the ffCO_2 concentrations are well reproduced by the estimated emissions. In Fig. 6 (bottom) we plot the wavelet coefficients obtained by projecting the emissions (both the true and reconstructed) on the wavelet bases. The wavelet coefficient values have been subjected to a hyperbolic tangent transformation for ease of plotting. The true wavelet coefficients with a magnitude above 0.01 are plotted with red symbols. The true (Vulcan) emissions have a large number of coefficients with small magnitude; these are usually for small-scale features i.e., have coefficient indices in the right half of the range (Fig. 6, bottom; red symbols). During sparse reconstruction, these coefficients are set to zero (blue symbols in Fig. 6, bottom). The low-index coefficients, which represent large structures, are estimated accurately. The explicit separation of scales is thus leveraged into ~~ignoring unimportant,~~ omitting fine-scale details which are difficult to inform with data and focusing model-fitting effort on the large scales instead. Sparse reconstruction achieves this in an automatic, purely data-driven manner, rather than via a pre-processing, scale-selection step.

Finally, we address the issue of enforcing the ~~$\mathbf{F}_{\mathcal{R}'} = 0$~~ $\boldsymbol{F}_{\mathcal{R}'} = 0$ constraint via random M_{cs} projections. Naively, the constraint can be enforced for every individual grid-cell, resulting in

$N_{\mathcal{R}'} = 3280$ linear equations per 8 day period in Eqs. (10) and (13). Considering that $\boldsymbol{y}^{\text{obs}} = \mathbf{H}\tilde{\mathbf{\Phi}}_{\mathcal{R}}$ results in $64 \times 35 = 3240$ linear equations per 8 day period, we see that enforcing the constraint is as expensive as computing ~~$\mathbf{F}_{\mathcal{R}}$~~ $\boldsymbol{F}_{\mathcal{R}}$. Instead, we set $M_{\text{cs}} \ll N_{\mathcal{R}'}$ random projections of ~~$\mathbf{F}_{\mathcal{R}'}$~~ $\boldsymbol{F}_{\mathcal{R}'}$ to zero in Eqs. (10) and (13), exploiting the basic efficiency-via-random-sampling tenet of CS. Since Eq. (13) is solved approximately, and due to the small number of wavelets in $W^{(s)}$ that span $\mathcal{R}'$, the constraint ~~$\mathbf{F}_{\mathcal{R}'} = 0$~~ $\boldsymbol{F}_{\mathcal{R}'} = 0$ is not satisfied exactly. This error varies with M_{cs}; a larger M_{cs} results in a closer realization of the constraint. Errors in the enforcement of the ~~$\mathbf{F}_{\mathcal{R}'} = 0$~~ $\boldsymbol{F}_{\mathcal{R}'} = 0$ constraint lead to commensurate errors in ~~$\mathbf{F}_{\mathcal{R}}$~~ $\boldsymbol{F}_{\mathcal{R}}$. Here we check the trade-off between M_{cs} (computational efficiency) and accuracy of the estimated emissions (~~$\mathbf{F}_{\mathcal{R}}$ and $\mathbf{F}_{\mathcal{R}'}$~~ $\boldsymbol{F}_{\mathcal{R}}$ and $\boldsymbol{F}_{\mathcal{R}'}$). In practice, this affects only Step I of the procedure, where an approximation of ffCO_2 emissions is calculated; thereafter it is used as a guess in Step II. However, a good estimate of the emission field accelerates the second step. The quality of the solution from Step I, quantified as the cumulative distribution function (CDF) of the fluxes can be found in Ray et al. (2013, 2014). There are only a few grid-cells with negative emissions and their magnitudes are small.

In Fig. 7, we plot the impact of M_{cs} on the reconstruction. We perform sparse reconstruction of the emission field, for the 31st 8 day periods and compute the ratios

$$\eta_{\mathcal{R}} = \frac{||\boldsymbol{f}_{k,\mathcal{R}}||_2}{||\boldsymbol{f}_{V,k}||_2} \text{ and } \eta_{\mathcal{R}'} = \frac{||\boldsymbol{f}_{k,\mathcal{R}'}||_2}{||\boldsymbol{f}_{V,k}||_2} \text{ for } k = 31. \tag{19}$$

Here $\boldsymbol{f}_{k,\mathcal{R}}$ and $\boldsymbol{f}_{k,\mathcal{R}'}$ are the emissions over $\mathcal{R}$ and $\mathcal{R}'$ from Step I. $\boldsymbol{f}_{V,k}$ is the true (Vulcan) emission field during the same period. These ratios are plotted as a function of $\log_{10}(M_{\text{cs}})$ per 8 day period. We see that 10 projections per 8 day period is too few, leading to around 20 % errors in $\boldsymbol{f}_{k,\mathcal{R}'}$ ($\eta_{\mathcal{R}'} \approx 0.2$). Beyond about 100 projections per 8 day period, $\eta_{\mathcal{R}'}$ oscillates around 0.1. The corresponding errors in $\boldsymbol{f}_{k,\mathcal{R}}$ are about 5 % ($\eta_{\mathcal{R}} \approx 1.05$). In our study we used 300 random projections for each 8 day period. This is about 10 % of the 3280 linear constraints that we would have enforced under a naive implementation of the ~~$\mathbf{F}_{\mathcal{R}'} = 0$~~ $\boldsymbol{F}_{\mathcal{R}'} = 0$ constraint. It also halves the computational cost of Step I.

5 Conclusions

In this study, we have developed a sparse reconstruction scheme that could be used for solving physics-based linear inverse problems. Our method is an extension of Stagewise Orthogonal Matching Pursuit (Donoho et al., 2012) and borrows many concepts from the compressive sensing (CS) and sparse reconstruction of images (Candes and Wakin, 2008). This scheme is useful for estimating non-stationary fields e.g., permeability or flux fields, provided their random field model consists of independent parameters. This is typically achieved by representing the fields in terms of orthogonal bases, e.g., wavelets or Karhunen–Loève modes, if a prior covariance is available. The dimensionality of the resultant representation is not an issue; the sparse reconstruction method estimates only those parameters that are informed by the observations while setting the rest to zero.

Our new method has three novel characteristics. Firstly, it can impose non-negativity on the estimated field, without resorting to log-transformations. This retains the linear nature of the inverse problem and consequently, its computational efficiency. Secondly, it allows one to estimate geometrically irregular fields while using a random field model designed for rectangular domains. Thirdly, it allows us to incorporate a prior model of the field being estimated into the sparse reconstruction procedure. While other model-based sparse reconstruction methods exist (Baraniuk et al., 2010; He and Carin, 2009; La and Do, 2005), our method is simple and is seen empirically to recover the correct solution.

We have demonstrated our method ~~on~~ in an atmospheric inverse problem for the estimation of a spatially rough emission field. It is an idealization of the estimation of $\mathrm{ffCO_2}$ emissions in $\mathcal{R}$, the lower 48 states of the US. The emissions were modeled in a square domain, with a 64×64 grid, using a recently developed Multiscale Random Field model (Ray et al., 2014). It uses Haar wavelets and images of lights at night to capture the spatial patterns of $\mathrm{ffCO_2}$ emission fields. The observational data consists of $\mathrm{ffCO_2}$ measurements at a limited set of towers, which are linked to the emission field via a $\mathrm{CO_2}$ transport model (the forward model). We draw parallels between our physics-based inverse problem and the sparse reconstruction of images in CS, and show that a fundamental CS tenet – incoherence – holds only approximately. Consequently,

such inverse problems may not bear an accurate solution if they are regularized solely using sparsity. We demonstrate this in our study and show how incorporation of prior information, in the form of spatial patterns in images of lights at night, and a prior model of $ffCO_2$ emissions can enable a solution. We also demonstrate how CS concepts can be used to restrict the estimated field to an irregular region (in our case, $\mathcal{R}$) with a factor-of-ten less computational effort than a naive approach. Finally, we show how non-negativity of $ffCO_2$ emissions can be imposed using a simple post-processing step.

~~We also considered bypassing Step I and estimating $\mathbf{E}$ (the non-negative emission field) directly using Step II , with $\mathbf{E}_0$~~ We also tested whether Step I (Sec. 3.2) was necessary by bypassing it completely, and starting Step II (Sec. 3.3) with $\boldsymbol{E}_0$ initialized using an inventory. We ~~find~~ do not present results of these tests in this paper, but find that the iterative scheme converges only when ~~$\mathbf{E}_0$~~ $\boldsymbol{E}_0$ is very close to the true results. For example, initializing using perturbed Vulcan emissions led a converged solution, whereas $\boldsymbol{f}_{\text{pr}}$ did not. Thus Step I is required for robustness and generality. This is particularly relevant for developing countries where inventories contain larger errors.

Our sparse reconstruction scheme suffers from one serious drawback - it does not provide uncertainty bounds on the estimated field due to the paucity of data, and/or the shortcomings of the models. While this can be rectified using a Kalman filter, it does not provide any mechanism for reducing the dimensionality of the random field model, should the observational data prove inadequate. This is currently being investigated. Also, we assumed that there were no emissions outside $\mathcal{R}$; in reality, there are. See our previous paper (Ray et al., 2014) on how they could be accommodated as boundary fluxes. Our use of the MsRF in the inversion is a second source of error; in the limit of a very informative measurement network, the accuracy of the inversion is limited by the ability of the MsRF to represent $ffCO_2$ fields accurately.

Due to the lack of a good tracer for $ffCO_2$ emissions, we demonstrated our method in an idealized inversion problem. The idealizations include a very small model - data mismatch ϵ (much smaller than what can be supported by contemporary transport models and radiocarbon measurement technology) and an ability to measure $ffCO_2$ accurately, without interference from biospheric CO_2 fluxes (i.e., we treated $ffCO_2$ like a radiocarbon tracer). In order that our

method could be used in a real-data inversion for $ffCO_2$ emissions, our method would need to be extended in a number of ways. First, we would require a measurement network better suited for $ffCO_2$ measurements, with sensors near large sources; one could be designed by conducting an OSSE (Observation System Simulation Experiment), perhaps using the method described here. Secondly, we would have to extend the method to perform a joint $ffCO_2$-biospheric CO_2 inversion, by including a spatial parameterization and priors for biospheric CO_2. Finally, we would have to devise a separate ϵ for each tower to reflect transport model errors.

In conjunction with this paper, we are also providing, at our website (Ray, 2013), the MATLAB® code required to construct the MsRF model for $ffCO_2$ emissions and perform the inversion using synthetic observations. The website also contains links to the (free) MATLAB® toolkits that our code depends on, along with a user' s manual.

Acknowledgements. This work was supported by Sandia National Laboratories' LDRD (Laboratory Directed Research and Development) funds, sponsored by the Geosciences Investment Area. Sandia National Laboratories is a multi-program laboratory managed and operated by Sandia Corporation, a wholly owned subsidiary of Lockheed Martin Corporation, for the US Department of Energy's National Nuclear Security Administration under contract DE-AC04-94AL85000.

References

Andres, R. J., Boden, T. A., Bréon, F.-M., Ciais, P., Davis, S., Erickson, D., Gregg, J. S., Jacobson, A., Marland, G., Miller, J., Oda, T., Olivier, J. G. J., Raupach, M. R., Rayner, P., and Treanton, K.: A synthesis of carbon dioxide emissions from fossil-fuel combustion, Biogeosciences, 9, 1845–1871, doi:10.5194/bg-9-1845-2012, 2012.

Babacan, S. D., Molina, R., and Katsaggelos, A. K.: Bayesian compressive sensing using Laplace priors, IEEE T. Signal Proces., 19, 55–63, doi:10.1109/TIP.2009.2032894, 2010.

Baraniuk, R., Davenport, M., DeVore, R., and Wakin, M.: A simple proof of the restricted isometry property for random matrices, Constr. Approx., 28, 253–263, 2008.

Baraniuk, R., Cevher, V., Duarte, M., and Hegde, C.: Model-based compressive sensing, IEEE T. Inform. Theory, 56, 1982–2001, 2010.

Candes, E. and Tao, T.: Near optimal signal recovery from random projections: universal encoding strategies?, IEEE T. Inform. Theory, 52, 5406–5425, 2006.

Candes, E. and Wakin, M.: An introduction to compressive sampling, IEEE Signal Proc. Mag., 25, 21–30, 2008.

Candes, E., Romberg, J., and Tao, T.: Robust uncertainty principles: exact signal reconstruction from highly incomplete frequency information, IEEE T. Inform. Theory, 52, 489–509, 2006.

~~Cand~~

Candés, E. and Romberg, J.: Sparsity and incoherence in compressive sampling, Inverse Probl., 23, 969, doi:10.1088/0266-5611/23/3/008, 2007.

Ciais, P., Rayner, P., Chevallier, F., Bousquet, P., Logan, M., Peylin, P., and Ramonet, M.: Atmospheric inversions for estimating CO_2 fluxes: methods and perspectives, Climate Change, 103, 69–92, 2010.

Cinzano, P., Falchi, F., Elvidge, C. D., and Baugh, K. E.: The artificial night sky brightness mapped from DMSP satellite Operational Linescan System measurements, Mon. Not. R. Astron. Soc., 318, 641–657, 2000.

Coifman, R., Geshwind, F., and Meyer, Y.: Noiselets, Appl. Comput. Harmon. A., 10, 27–44, doi:10.1006/acha.2000.0313, 2001.

Donoho, D.: Compressed sensing, IEEE T. Inform. Theory, 52, 1289–1306, 2006.

Donoho, D. L., Tsaig, Y., Drori, I., and Starck, J.-L.: Sparse solution of underdetermined linear equations by stagewise orthogonal matching pursuit, IEEE T. Inform. Theory, 58, 1094–1121, 2012.

Duarte, M. F., Wakin, M. B., and Baraniuk, R. G.: Fast reconstruction of piecewise-smooth signals from random projections, in: Proceedings of Signal Processing with Adaptive Sparse Structured Representations, Rennes, France, 2005.

Gan, L., Do, T., and Tran, T.: Fast compressive imaging using scrambled block Hadamard ensemble, 16th European Signal Processing Conference, 2008.

Gerbig, C., Dolman, A. J., and Heimann, M.: On observational and modelling strategies targeted at regional carbon exchange over continents, Biogeosciences, 6, 1949–1959, doi:10.5194/bg-6-1949-2009, 2009.

Gholami, A. and Siahkoohi, H. R.: Regularization of linear and nonlinear geophysical ill-posed problems with joint sparsity priors, Geophys. J. Int., 180, 871–882, 2010.

Gourdji, S. M., Mueller, K. L., Yadav, V., Huntzinger, D. N., Andrews, A. E., Trudeau, M., Petron, G., Nehrkorn, T., Eluszkiewicz, J., Henderson, J., Wen, D., Lin, J., Fischer, M., Sweeney, C., and Michalak, A. M.: North American CO_2 exchange: inter-comparison of modeled estimates with results from a fine-scale atmospheric inversion, Biogeosciences, 9, 457–475, doi:10.5194/bg-9-457-2012, 2012.

Gurney, K. R., Mendoza, D. L., Zhou, Y., Fischer, M. L., Miller, C. C., Geethakumar, S., and de la Rue de Can, S.: High resolution fossil fuel combustion CO_2 emission fluxes in the United States, Environ. Sci. Technol., 43, 5535–5541, 2009.

He, L. and Carin, L.: Exploiting structure in wavelet-based bayesian compressive sensing, IEEE T. Signal Proces., 57, 3488–3497, 2009.

Hirst, B., Jonathan, P., del Cueto, F. G., Randell, D., and Kosut, O.: Locating and quantifying gas emission sources using remotely obtained concentration data, Atmos. Environ., 74, 141–158, 2013.

Jafarpour, B.: Sparsity-promoting solution of subsurface flow model calibration inverse problems, in: Advances in Hydrogeology, edited by: Mishra, P. K. and Kuhlman, K. L., Springer, 2013.

Ji, S., Xue, Y., and Carin, L.: Bayesian compressive sensing, IEEE T. Signal Proces., 56, 2346–2356, doi:10.1109.TSP.2007.914345, 2008.

Kort, E. A., Frankenberg, C., Miller, C. E., and Oda, T.: Space-based observations of megacity carbon dioxide, Geophys. Res. Lett., 39, ~~L19806~~4493, doi:10.1029/2002JD003161, 2012.

La, C. and Do, M. N.: Signal reconstruction using sparse tree representation, in: Proc. Wavelets XI at SPIE Optics and Photonics, San Diego, CA, USA, 2005.

Li, L. and Jafarpour, B.: A sparse Bayesian framework for conditioning uncertain geologic models to nonlinear flow measurements, Adv. Water Resour., 33, 1024–1042, 2010. in list

Lin, J. C., Gerbig, C., Wofsy, S. C., Andrews, A. E., Daube, B. C., Davis, K. J., and Grainger, C. A.: A near-field tool for simulating the upstream influence of atmospheric observations: the Stochastic Time-Inverted Lagrangian Transport (STILT) model, J. Geophys. Res., 108, 4493, doi:10.1029/2002JD003161, 2003.

Loris, I., Nolet, G., Daubechies, I., and Dahlen, F. A.: Tomographic inversion using ℓ_1-norm regularization of wavelet coefficients, Geophys. J. Int., 170, 359–370, 2007.

Mallat, S. and Zhang, Z.: Matching pursuit with time-frequency dictionaries, IEEE T. Signal Proces., 41, 3397–3415, 1993.

Martinez-Camara, M., Dokmanic, I., Ranieri, J., Scheibler, R., M. Vetterli, M., and Stohl, A.: The Fukushima inverse problem, in: 2013 IEEE International Conference on Acoustics, Speech and Signal Processing (ICASSP), 4330–4334, 2013.

McKain, K., Wofsy, S., Nehrkorn, T., Eluszkiewicz, J., Ehrlinger, J. R., and Stephens, B. B.: Assessment of ground-based atmospheric observations for verification of greenhouse gas emissions from an urban region, P. Natl. Acad. Sci. USA, 109, 8423–8428, 2012.

Oda, T. and Maksyutov, S.: A very high-resolution ($1\,\mathrm{km} \times 1\,\mathrm{km}$) global fossil fuel CO_2 emission inventory derived using a point source database and satellite observations of nighttime lights, Atmos. Chem. Phys., 11, 543–556, doi:10.5194/acp-11-543-2011, 2011.

Olivier, J. G. J., Aardenne, J. A. V., Dentener, F. J., Pagliari, V., Ganzeveld, L. N., and Peters, J. A. H. W.: Recent trends in global greenhouse gas emissions: regional trends 1970–2000 and spatial distribution of key sources in 2000, Journal of Integrative Environmental Science, 2, 81–99, 2005.

Pacala, S. W., Breidenich, C., Brewer, P. G., Fung, I. Y., Gunson, M. R., and co authors: Verifying Greenhouse Gas Emissions: Methods to Support International Climate Agreements, Committee on Methods for Estimating Greenhouse Gas Emissions, National Research Council, The National Academies Press, available at: http://www.nap.edu/openbook.php?record_id=12883 (last access: 13 August 2014), 2010.

Potter, C. S., Randerson, J. T., Field, C. B., Matson, P. A., Virousek, P. M., Mooney, H. A., and Klooster, S. A.: Terrestrial ecosystem production: a process model based on global satellite and surface data, Global Biogeochem. Cy., 7, 811–841, 1993.

Ray, J.: Estimating $\mathrm{ffCO_2}$ using a MsRF and sparse reconstruction, available at: http://www.sandia.gov/~jairay/software.html (last access: 13 August 2014), 2013.

Ray, J., Lee, J., Lefantzi, S., Yadav, V., Michalak, A. M., Bloemen-Waanders, B., and McKenna, S. A.: A multiresolution spatial parametrization for the estimation of fossil-fuel carbon dioxide emissions via atmospheric inversions, SAND Report SAND2013-2919, Sandia National Laboratories, Livermore, CA 94551-0969, available at: http://www.sandia.gov/~jairay/Presentations/sand2013-2919.pdf (last access: 13 August 2014), unclassified and unlimited release, 2013.

Ray, J., Yadav, V., Michalak, A. M., van Bloemen Waanders, B., and McKenna, S. A.: A multiresolution spatial parameterization for the estimation of fossil-fuel carbon dioxide emissions via atmospheric inversions, Geosci. Model Dev. Discuss., 7, 1277–1315, doi:10.5194/gmdd-7-1277-2014, 2014.

Rayner, P. J., Raupach, M. R., Paget, M., Peylin, P., and Koffi, E.: A new global gridded data set of CO_2 emissions from fossil fuel combustion: methodology and evaluation, J. Geophys. Res., 115, D19306, doi:10.1029/2009JD013439, 2010.

Romberg, J.: Imaging via compressive sampling, IEEE Signal Proc. Mag., 25, 14–20, 2008.

Simons, F. J., Loris, I., Nolet, G., Daubechies, I. C., Voronin, S., Judd, J. S., Vetter, P. A., Vetter, P. A., Charlety, J., and Vonesch, C.: Solving or resolving global tomographic models with spherical wavelets and the scale and sparsity of seismic heterogeneity, Geophys. J. Int., 187, 969–988, 2011.

Skamarock, W. C. and Klemp, J. B.: A time-split nonhydrostatic atmospheric model for weather research and forecasting applications, J. Comput. Phys., 227, 3465–3485, 2008. in list

Tans, P. and Conway, T. J.: Monthly atmospheric CO_2 mixing ratios from the NOAA CMDL Carbon Cycle Cooperative Global Air Sampling Network, 1968–2002, in: Trends: A Compendium of Data on Global Change, Carbon Dioxide Information Analysis Center, Oak Ridge National Laboratory, Oak Ridge, TN, 2005.

Tropp, J. and Gilbert, A. C.: Signal recovery from partial information via orthogonal matching pursuit, IEEE T. Inform. Theory, 53, 4655–4666, 2007.

Tsaig, Y. and Donoho, D.: Extensions of compressed sensing, Signal Process., 86, 533–548, 2006.

Tuma, T. and Hurley, P.: On the incoherence of noiselet and Haar bases, in: International Conference on Sampling Theory and Applications, 2009.

Turnbull, J. C., Karion, A., Fischer, M. L., Faloona, I., Guilderson, T., Lehman, S. J., Miller, B. R., Miller, J. B., Montzka, S., Sherwood, T., Saripalli, S., Sweeney, C., and Tans, P. P.: Assessment of fossil fuel carbon dioxide and other anthropogenic trace gas emissions from airborne measurements over Sacramento, California in spring 2009, Atmos. Chem. Phys., 11, 705–721, doi:10.5194/acp-11-705-2011, 2011.

Yin, W., Morgan, S., Yang, J., and Zhang, Y.: Practical compressive sensing with Toeplitz and circulant matrices, in: Proc. SPIE, 7744, 77 440K-77 440K-10, doi:10.1117/12.863527, 2010.

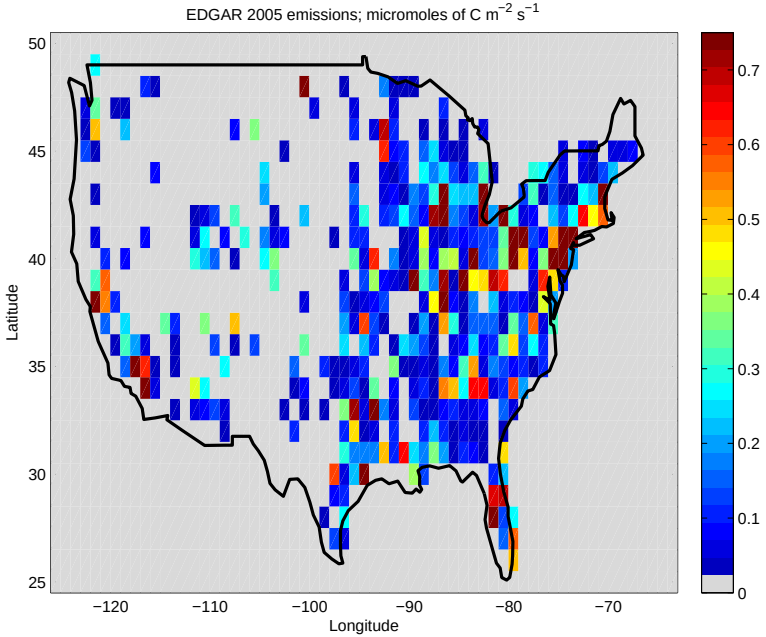

Figure 1. Plot of US $ffCO_2$ emissions (micromoles of C m^{-2} s^{-1}) as reported by EDGAR for 2005. Emissions below 0.02 micromoles of C m^{-2} s^{-1} are grayed out.

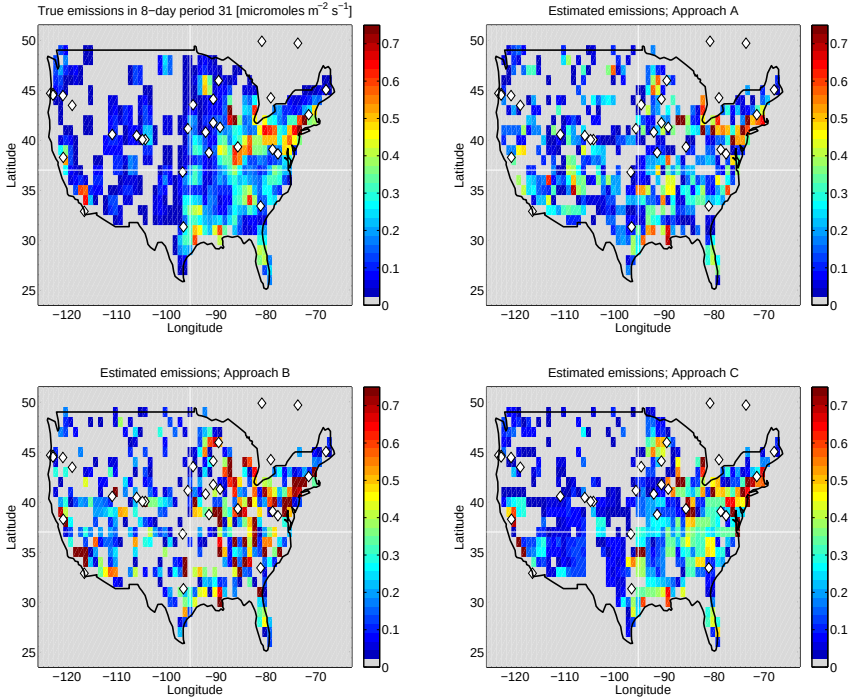

Figure 2. Plots of $\mathrm{ffCO_2}$ emissions during the 31st 8 day period. The units are micromoles of C $\mathrm{m^{-2}\ s^{-1}}$. Emissions below 0.02 micromoles of C $\mathrm{m^{-2}\ s^{-1}}$ are grayed out. Top left, we plot true emissions from the Vulcan inventory. Top right, the estimates from Approach A. Bottom left and right figures contain the estimates obtained from Approaches B and C respectively. Each figure contains the measurement towers as white diamonds. Each figure is also divided into quadrants. We see that Approach A, unconstrained by $\boldsymbol{f}_{\mathrm{pr}}$ provides low levels of (erroneous) emissions in large swathes of the Western quadrants. Approach B reflects $\boldsymbol{f}_{\mathrm{pr}}$ very strongly. Approach C provides a balance between the influence of $\boldsymbol{f}_{\mathrm{pr}}$ and the information in $\boldsymbol{y}^{\mathrm{obs}}$.

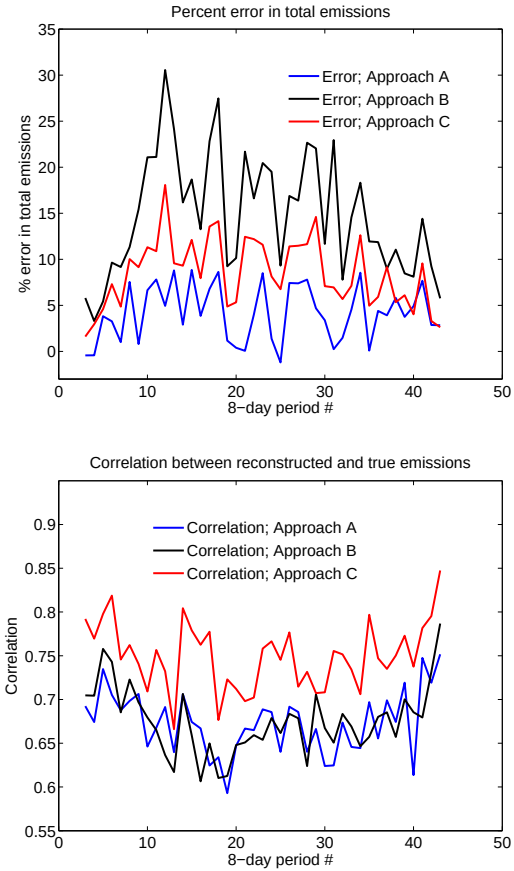

Figure 3. Comparison of estimation error (left) and the correlation between true and estimated emissions (right) using Approaches A, B and C. It is clear that Approach B is inferior to the others.

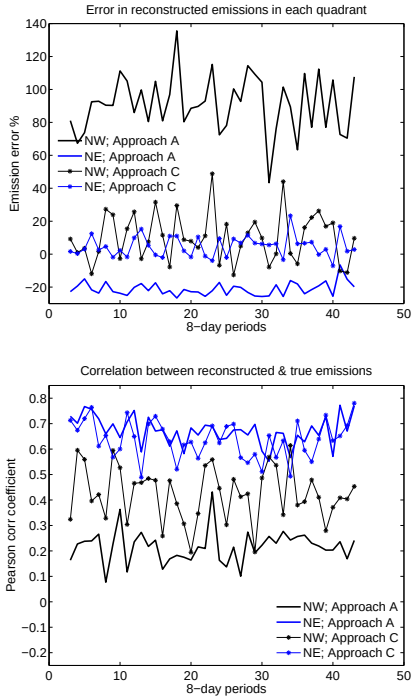

Figure 4. Reconstruction error (left) and correlation between the true and estimated emissions, using Approaches A and C, for the Northeast (NE) and Northwest (NW) quadrants. We see that Approach C, which includes information from $\boldsymbol{f}_{\text{pr}}$, leads to lower errors in both the quadrants and better correlations in the less instrumented NW quadrant.

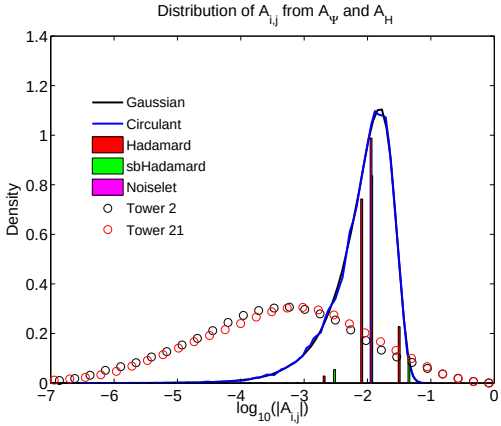

Figure 5. Comparison of the distribution of the elements of $\mathbf{A_\Psi}$ and $\mathbf{A_\Phi}$. We see that Gaussian and circulant random matrices lead to continuous distributions whereas Hadamard, scrambled-block Hadamard (sbHadamard) and noiselets serving as sampling matrices lead to $\mathbf{A_\Psi}$ where the elements assume discrete values. In contrast, the elements of $\mathbf{A_{H'}}$ assume values which are spread over a far larger range, some of which are quite close to 1 while others are very close to zero.

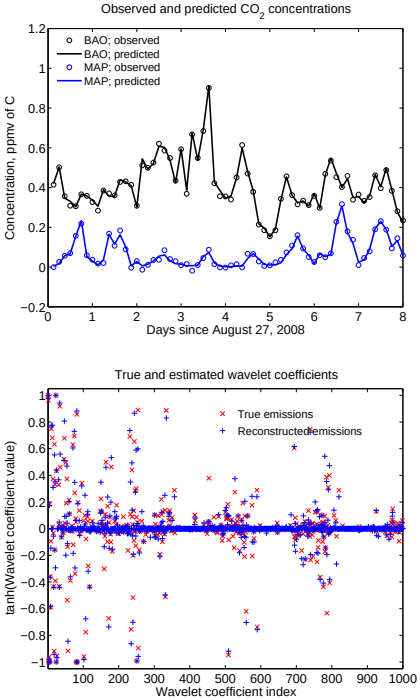

Figure 6. Top: predictions of $ffCO_2$ concentrations at 2 measurement locations, using the true (Vulcan) and reconstructed emissions (blue lines) over an 8 day period (Period no. 31). Observations occur every 3 h. We see that the concentrations are accurately reproduced by the estimated emissions. Below: projection of the true and estimated emissions on the wavelet bases for the same period. Coarse wavelets have lower indices, and they progressively get finer with the index number. We see that the true emissions have a large number of wavelets with small, but not zero, coefficients. In the reconstruction (plotted in blue), a number of wavelet coefficients are set to very small values (almost zero) by the sparse reconstruction. The larger scales are estimated accurately.

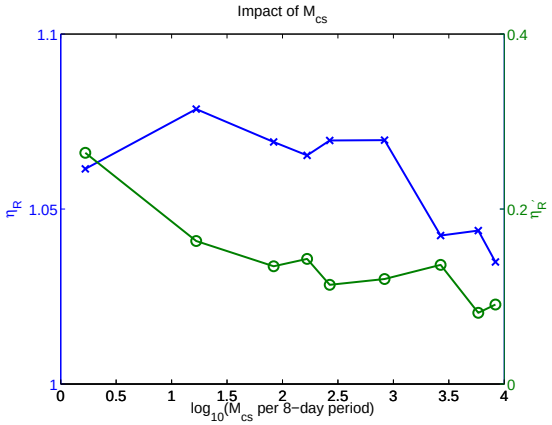

Figure 7. The impact of the number of compressive samples M_{cs} on the reconstruction of ~~$\mathbf{F}_{\mathcal{R}}$~~ $\boldsymbol{F}_{\mathcal{R}}$ ($\eta_{\mathcal{R}}$) and ~~$\mathbf{F}_{\mathcal{R}'}$~~ $\boldsymbol{F}_{\mathcal{R}'}$ ($\eta_{\mathcal{R}'}$). $\eta_{\mathcal{R}}$ and $\eta_{\mathcal{R}'}$ are plotted on the Y1 and Y2 axes respectively. Results are plotted for the 31st 8 day period. We see that $M_{\text{cs}} > 10^3$ does not result in an appreciable increase in reconstruction quality. Also, $M_{\text{cs}} < 10^2$ shows a marked degradation in $\eta_{\mathcal{R}'}$.